A literature review on pharmacological aspects, docking studies, and synthetic approaches of quinazoline and quinazolinone derivatives

Mohammed M. Ghoneim[1], Mohamed A. Abdelgawad[2*], Nadia A. A. Elkanzi[3], Della Grace Thomas Parambi[2],Izzeddin Alsalahat[4], Amr Farouk[5], Rania B. Bakr[6*]

[1]Department of Pharmacy Practice, College of Pharmacy, AlMaarefa University, Ad Diriyah 13713, Saudi Arabia. (mghoneim@um.edu.sa).

[2]Department of Pharmaceutical Chemistry, College of Pharmacy, Jouf University, Sakaka 72431, Saudi Arabia; (DGTP, dellajesto@ju.edu.sa; MAA, mhmdgwd@ju.edu.sa).

[3]Department of Chemistry, College of Science, Jouf University, Sakaka, 2014, Saudi Arabia (nahasan@ju.edu.sa).

[4]UK Dementia Research Institute Cardiff, School of Medicine, Cardiff University, Cardiff CF24 1TP, UK (Alsalahati@cardiff.ac.uk).

[5]Flavour and Aroma Chemistry Department, National Research Centre, Dokki, Cairo, 12622, Egypt (af.mansour@nrc.sci.eg)

[6]Pharmaceutical Organic Chemistry Department, Faculty of Pharmacy, Beni-Suef University, Beni-Suef, 62514, Egypt(raniabakr@ymail.com)

Corresponding authors (RBB, raniabakr@ymail.com)

(MAA, mhmdgwd@ju.edu.sa)

Abstract

Quinazoline and quinazolinone derivatives piqued medicinal chemistry interest in developing novel drug candidates owing to their pharmacological potential.

They are important chemicals for the synthesis of a variety of physiologically significant and pharmacologically useful molecules. Quinazoline and quinazolinone derivatives have anticancer, anti-inflammatory, antidiabetic, anticonvulsant, antiviral and antimicrobial potential. The increased understanding of quinazoline and quinazolinone derivatives in biological activities provides opportunities for new medicinal products. The present review focuses on novel advances in the synthesis of these important scaffolds and other medicinal aspects involving drug design, structure-activity relationship (SAR), and action mechanisms of quinazoline and quinazolinone derivatives to help in the development of new quinazoline and quinazolinone derivatives.

Keywords: Quinazoline, quinazolinone, anticancer, anti-inflammatory, antidiabetic antimicrobial.

1. Introduction

Quinazoline is a nitrogen-containing compound with a fused heterocycle known as benzo[*a*]pyrimidine, 5,6-benzopyrimidine, and / or phenmiazine and its 4-oxo derivative which is known as 4(3*H*)quinazolinones [1, 2]. Quinazoline scaffold has four isomers, namely, cinnoline, phthalazine, quinoxaline and, quinazoline [3-6]. Carbonyl linkage on the quinazoline ring will produce quinazolinone (4(3*H*)-quinazolinone & 2(1*H*)-quinazolinone.

Quinazoline and quinazolinone heterocycles are one of the most promising scaffolds because of their stability, ease of synthetic accessibility, and flexibility in structural modification and functionalization. The lipophilicity of these heterocycles is another cause for this interest since it helps quinazoline and quinazolinone to penetrate blood-brain barrier making them suitable for various CNS diseases. Many available drugs are dependent on quinazoline and quinazolinone scaffold. They are recorded to exhibit diverse biological potentials as anti-inflammatory [7, 8], anticancer [9-12], antidiabetic [13, 14], antihypertensive [15], antimalarial [16], antimicrobial [17-19], antiviral [20, 21], anticonvulsant[22-24], anticholine esterase [25-27] and antioxidant [28, 29].

Quinazolinone derivatives were building blocks for nearly 150 alkaloidal metabolites isolated from various families of plants, animals, and microorganisms [30, 31].

There are many synthetic and natural-based drugs incorporating quinazoline and quinazolinone moieties which are utilized for curing many diseases [32-34] (Fig. 1).

Hybrid compounds having quinazoline/ quinazolinone scaffolds and other biologically active heterocycles could contribute to drugs with decreased drug resistance and enhanced pharmacological potential [35-37].

This review reveals medicinal chemistry efforts in the search for novel quinazolines and quinazolinones that are of potential biological activity with an emphasis on the

SAR and the synthetic methods utilized for the synthesis of these heterocycles from 2010 to date.

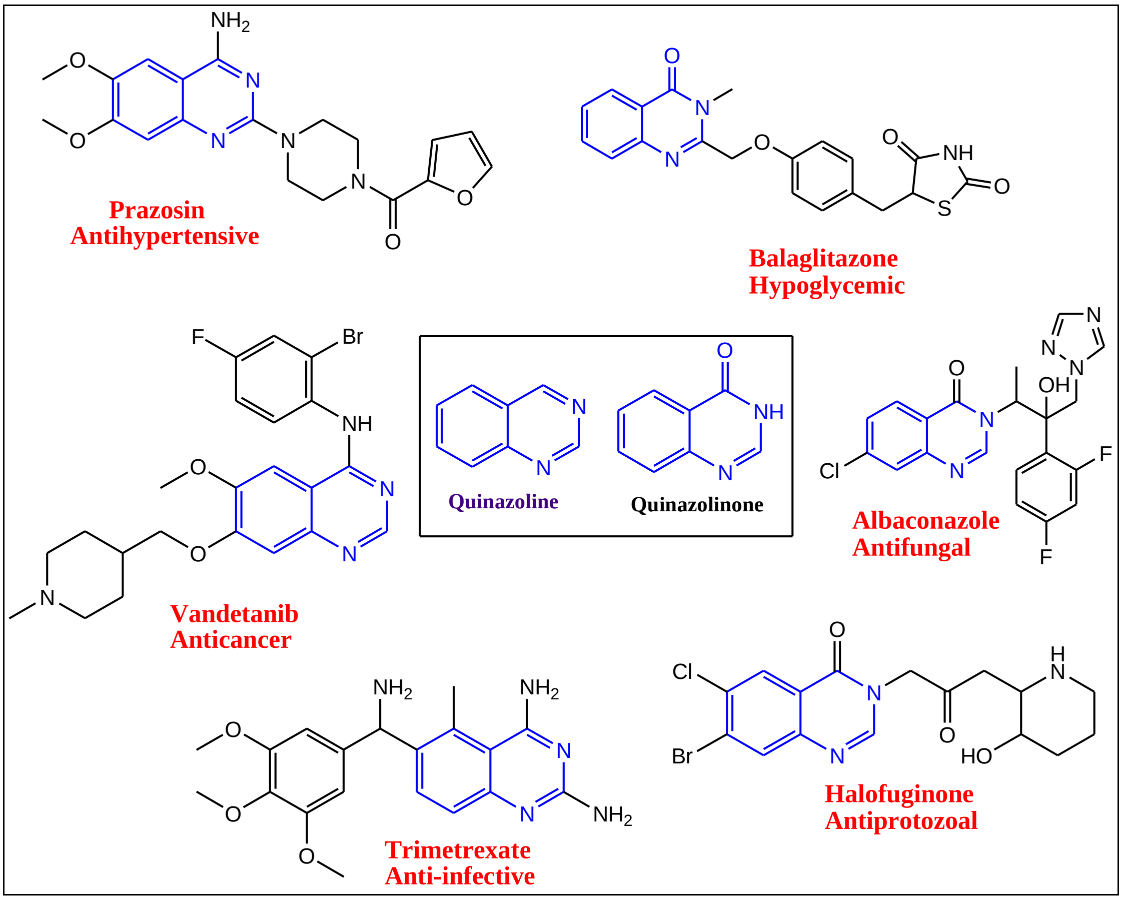

Fig.1. Chemical structures of some quinazolines and quinazolinones with pharmacological potential.

2. Synthetic routes of quinazoline derivatives

2,4-Disubstitutedquinazoline derivatives were prepared through different pathways as revealed in Fig. 2. 4-Phenylquinazoline derivatives were prepared through Friedel Crafts cyclization of arylguanidines**I** in [OMIm]X ionic liquid under microwave irradiation for 10 min (Pathway A) [38]. Moreover, quinazolines were synthesized from the isomerization of the Pd-alkene complex intermediate of *N*-allylamidines**II** in the presence of palladium acetate at 170^{o}C under microwave irradiation [39] (Pathway B). Furthermore, cyclizing 2-aminophenylcarbonyl compounds **III** with nitriles in the presence of trimethylsilylrifluoromethanesulfonate (TMSOFOT) under microwave irradiation at 100°C for 10 min furnished quinazoline derivatives [40] (Pathway C). In addition, treating *o*-fluorobenzonitriles (**IV**) with S-alkylisothiouronium salts at 120°C for 5-30 min in basic alumina-furnished 2-alkylthio-4-aminoquinazolines [41] (Pathway D). In addition, quinazolines were synthesized through one-pot three-component reactions of 2-aminobenzophenones (**V**), urea, and the appropriate aromatic aldehydes [42] (Pathway E).

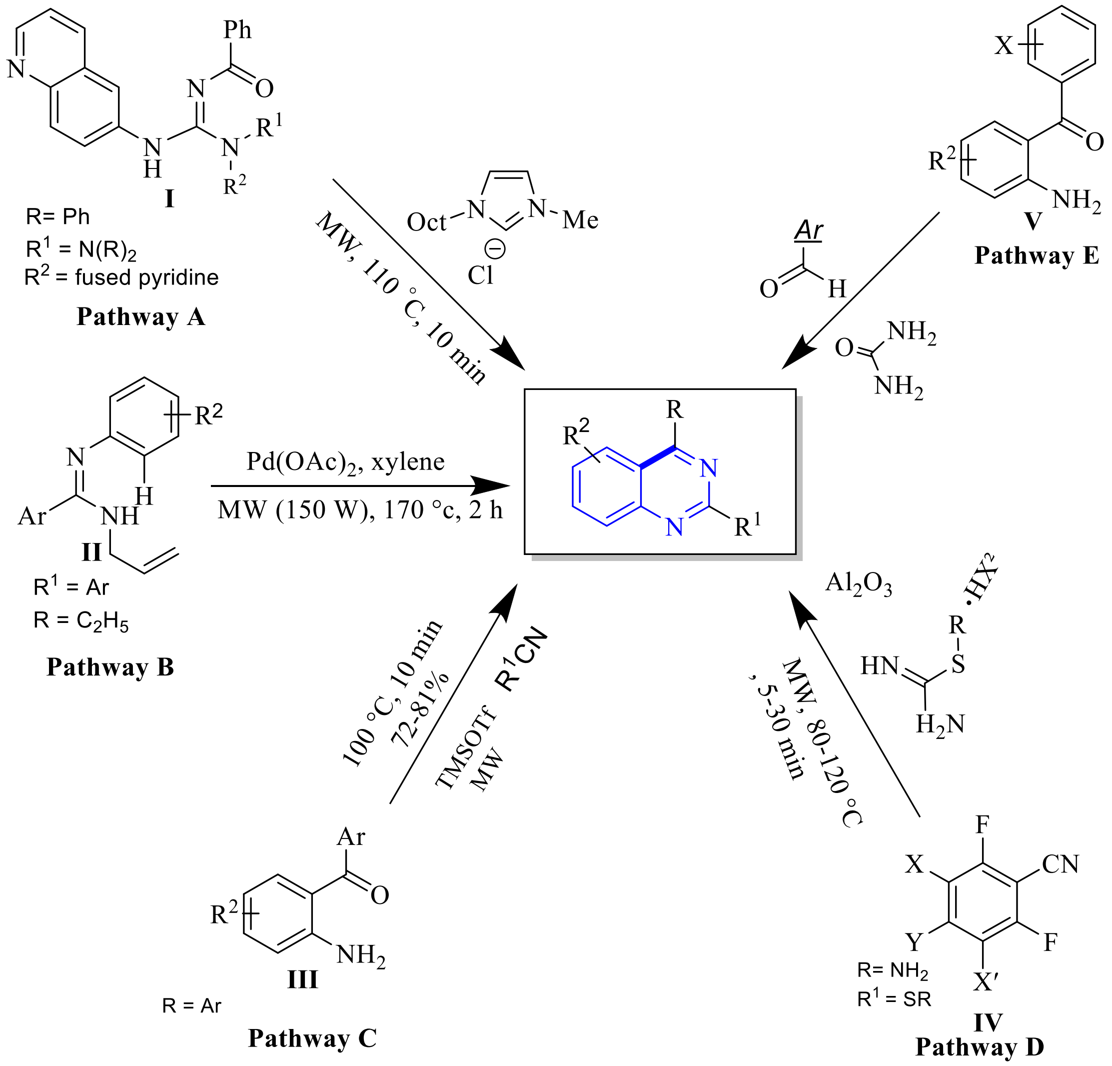

Fig.2. Synthetic methods for 2,4-disubstitutedquinazoline derivatives.

4-Substitutedquinazoline derivatives were synthesized *via* many procedures as depicted in Fig. 3. Reacting thiourea with **VI** in DMSO at 150°C for 4-6 h furnished 4-arylquinazoline derivatives (Pathway F) [43]. Moreover, In 2014, Foucourt *et al*[44] synthesized thiazolo[5,4-*f*]quinazoline-2-carbonitriles starting from 2-amino-5-nitroanthranilonitrile (**VII)** which was reacted with dimethylformamide dimethyl acetal (DMF-DMA) under microwave irradiation at 105^{o}C for 15 min followed by heating the formed *N*,*N*-dimethylformamidine**VIII** with the appropriate amines in acetic acid for 20 min at 118 ^{o}C (Pathway G). Treating 5-nitroanthranilonitrile (**IX**) with DMF-DMA for 2 min under microwave irradiation at 70^{o}C produced the *N*,*N*-dimethylformamidine derivative (**X**) which was cyclized to 6-nitro-4-(3-bromophenylamino)quinazoline through the reaction with an appropriate aniline in acetic acid at 118^{o}C under microwave irradiation (Pathway H) [45]. Moreover, quinazoline-4-ylaminomethylphosphonate was synthesized in high yield *via* reacting amidines **XI** with dialkylaminophenylmethylphosphonates under microwave irradiation using isopropyl alcohol and acetic acid at 100^{o}C for 20 min (Pathway I) [46].

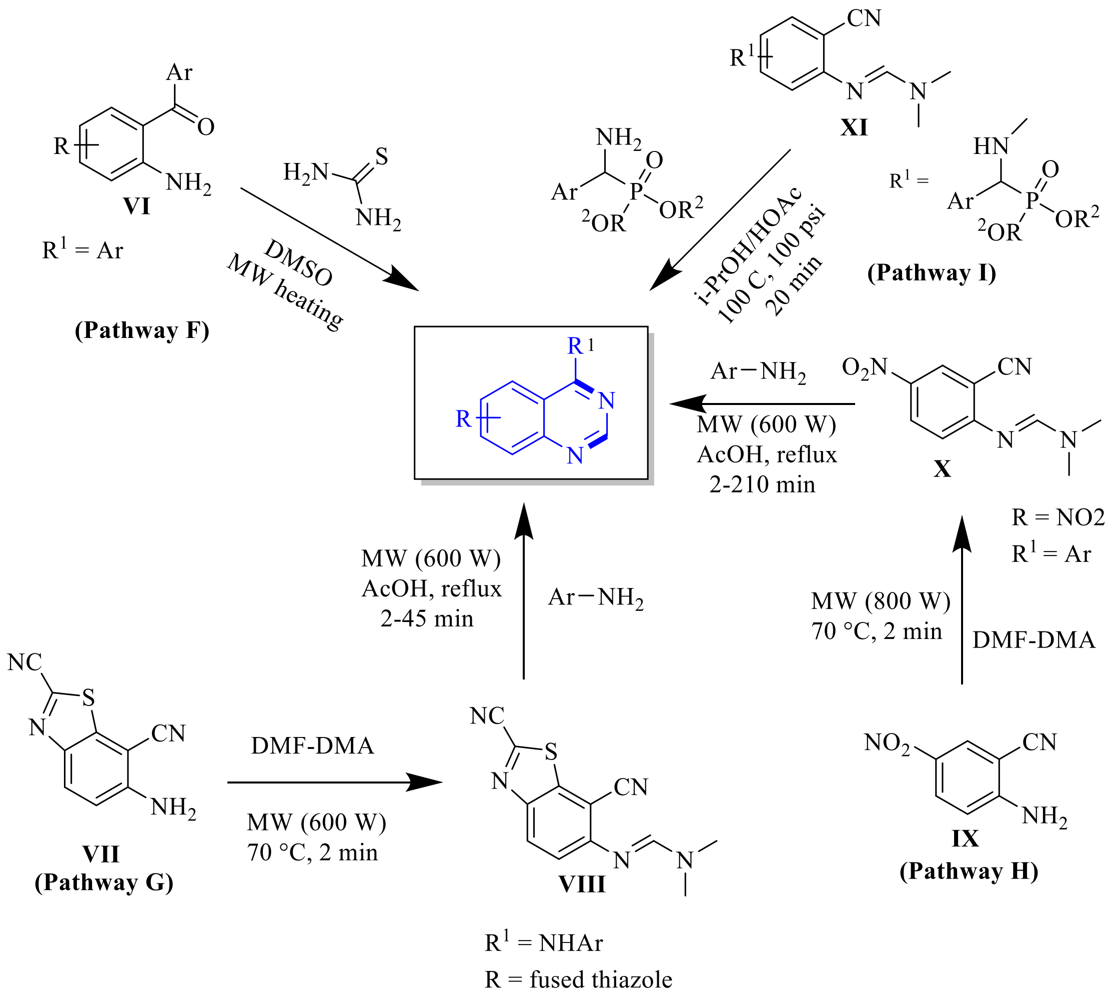

Fig.3. Synthetic methods for 4-substitutedquinazoline derivatives.

Regarding the preparation of quinazolinone derivatives, several methods could be applied in Fig. 4. For example, the reaction of various *o*-nitrobenzamides **XII** and aryl iodide utilizing palladium catalyst yielded 2-substituted quinazolinone derivatives (Pathway J) [47] (Fig. 4). In addition, quinazolinone derivative was synthesized from cyclocondensation of azido or nitrobenzoic acids **XIII** employing Zn-HCO_2NH_4 under microwave irradiation at 300 W (Pathway K) [48]. Furthermore, quinazolinone derivatives were prepared *via* coupling substituted 2-halobenzoic acid **XIV** with amidines in the presence of cupric chloride, ligand, and sodium hydroxide using microwave irradiation for 20 min (Pathway L) [49]. On the other hand, Pd-catalyzed hydrogenation of *o*-nitrobenzamides**XV** using a triethylamine-formic acid mixture

(TEAF) produced quinazolin-4(3*H*)-one derivative under microwave irradiation at 150 °C for 8 min (Pathway M) [50]. The reaction between *N*-acetylanthranilic acids **XVI** with 4-acetamidobenzenesulfonyl hydrazide using PCl_3 in tetrahydrofuran under microwave irradiations formed quinazolinones (Pathway N) [51].

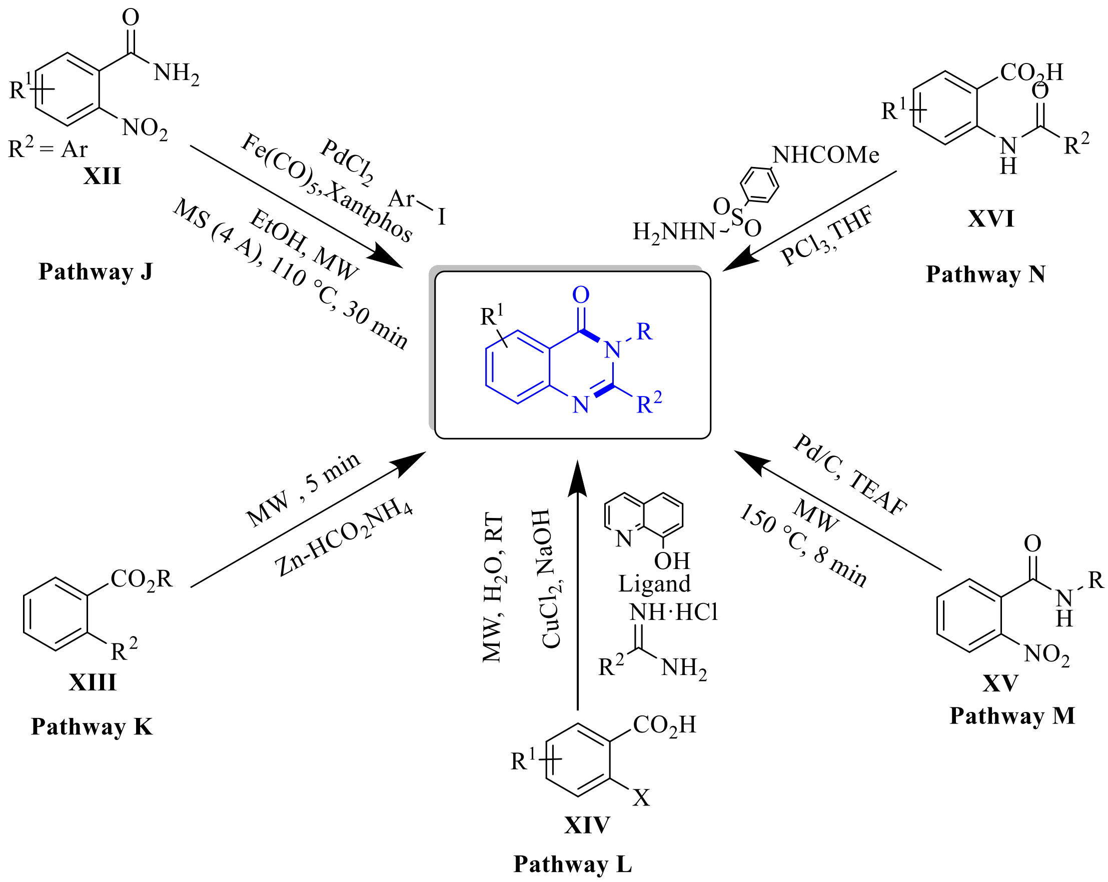

Fig.4. Synthetic methods for 4-quinazolinone derivatives.

On the other hand, anthranilic acid **XVII** was reported as a starting material for the preparation of quinazolinone derivatives *via* several methods as illustrated in Fig. 5. Condensation of anthranilic acid (**XVII**) with thiocarbamate salt of aniline derivatives using microwave irradiation in ethanol or under solvent-free condition furnished thioquinazolinone derivatives (Pathway O)[52]. Another method involved the synthesis of fluorine-containing quinazolinones utilizing anthranilic acid (**XVII**), trimethyl orthoformate and fluorinated anilines in absence of catalysts or solvents (Pathway P)[53]. Furthermore, novel series of 4-(3*H*)quinazolinone derivatives were synthesized *via* the reaction of anthranilic acid (**XVII**) with Vilsmeier reagent ($POCl_3$/ DMF) followed by cyclization with different substituted anilines (Pathway Q)[54]. Besides, another strategy for preparing quinazolinone was achieved from anthranilamide **XVIII** *via* condensation with different aromatic aldehydes in the presence of PTSA in polyethylene glycol (PEG-200/400) as a green solvent under microwave irradiations for 5-10 min (Pathway R) [55]. Also, reacting anthranilamide **XVIII** with potassium isopropyldithiocarbonate in DMF under solvent-free conditions afforded 2-mercaptoquinazolinone derivative (Pathway S)[56]. Furthermore, 2,3-disubstituted-4(3*H*)-quinazolinones were synthesized through a three-component reaction between isatoic anhydride (**XIX**), amines and, ortho-esters (Pathway T) [57].

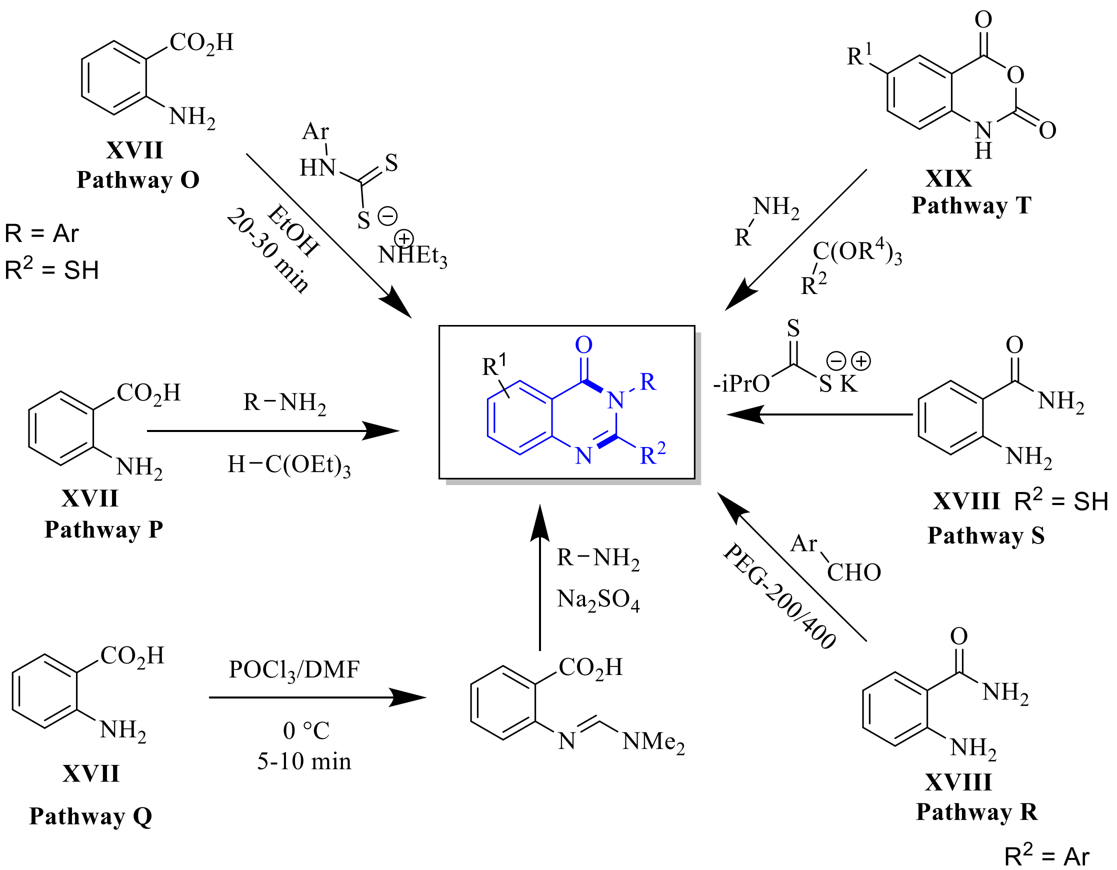

Fig. 5. Synthetic strategies for preparation of 4-quinazolinone derivatives.

3. Biological importance of quinazolines and quinazolinones

3.1. Anticancer activity

Many anticancer drugs with quinazoline scaffold have been discovered in the last decade. Gefitinb (**1**) and Erlotinib (**2**) (Fig. 6) are two significant anticancer drugs belonging to this group, released onto the market for treating non-small cell lung cancer (NSCLC) [11, 58, 59].

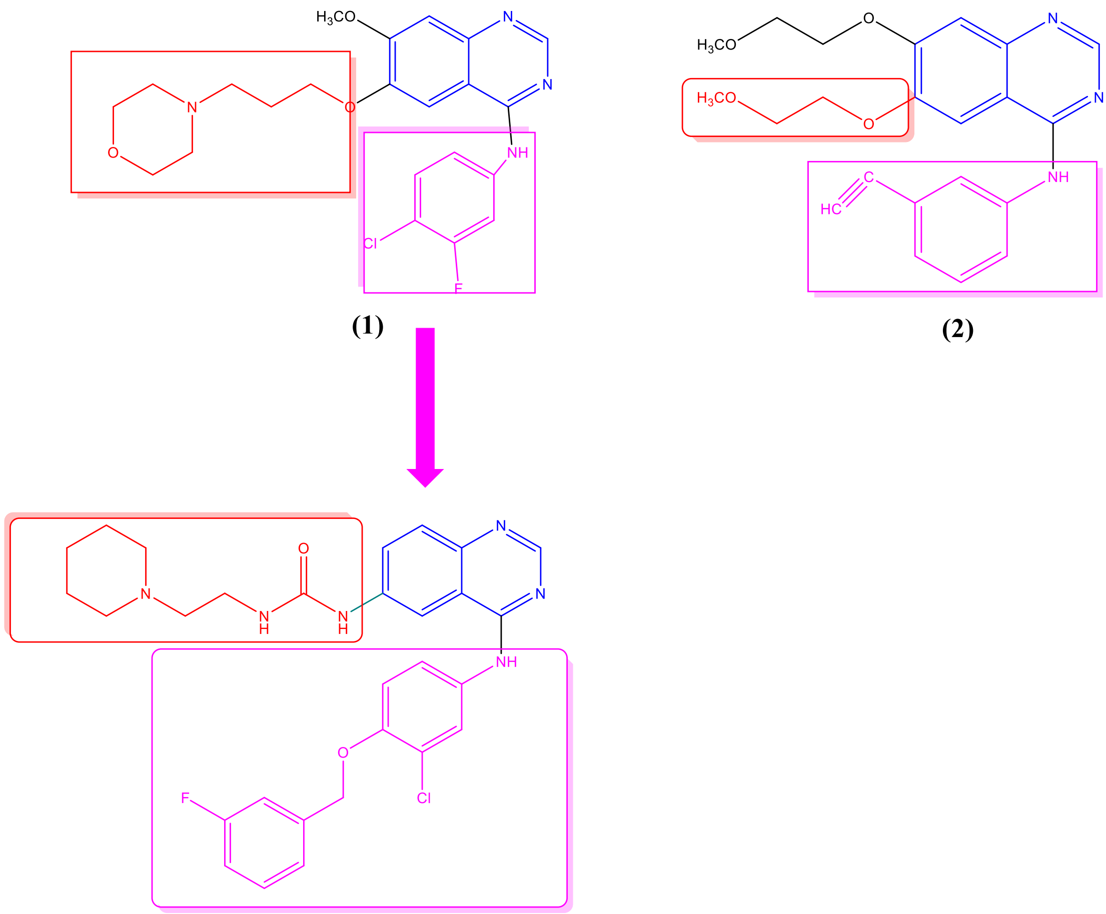

(1) **(2)** **(3)**

Fig. 6. Chemical structures of Gefitinib **(1),** Erlotinib **(2)** and compound **3** as anticancer agents.

In 2016, novel series of quinazolines with ureido and thioureido moiety at C-6 and many substituents at C-4 anilino fragments were synthesized [60]. The rationale of this study depended on performing some modifications to the chemical structure of gefitinib. These modifications comprise adding different urea and thiourea at C-6 of the quinazoline ring as extra hydrogen bond acceptors and making different substitution patterns at the 4-anilino position (Fig. 6). Evaluation of these compounds towards the wild type (WT) and mutant EGFR inhibition demonstrated that most of the tested quinazolines exhibited EGFR kinase wild type (EGFR WT) inhibition with IC_{50} values in a low nanomolar range (IC_{50} = 0.495-9.05 nM). Compound **3** (Fig. 6) recorded excellent inhibition in these mutant lines (IC_{50} = 2.38 µM). In addition, growth inhibition by compound **3** (IC_{50} = 2.157 µM) towards gefitinib insensitive cell lines PC9-GR4 (Del19/T790M) recorded eight folds greater potency than gefitinib (IC_{50} = 16.33 µM). SAR study recorded the importance of ethyl piperidino urea/thiourea at C-6 and the bulky group of (3-chloro-4(3-fluorobenzyloxy) phenyl) amino at C-4 of quinazoline in potency towards resistant double mutant cell lines.

In 2019, Ansari *et al*[61]synthesized novel series of pyrazolo[1,5-*c*]quinazoline derivatives were synthesized and screened these compounds for their anticancer potential towards cancer cell lines TNBC, A549 and, H1299 by applying MTT assay. In this work, authors designed the novel compounds by replacing one of $COOCH_3$ groups of compounds **4** with small polar substituent NH_2 (Fig. 7). Compounds **5a,b** (< 2.5 µM) showed excellent anticancer activity compared with Gefitinib and Erlotinib (Table 1). Compounds **5a-c** were assessed for their EGFR inhibitory potential and the results showed that compounds **5a, b** mostly displayed EGFR inhibition with IC_{50} = 165.38 and 157.63 nM, respectively, in comparison to Erlotinib (IC_{50} = 201.34 nM). In silico binding of compounds **5a-c** within EGFR revealed that the hydrogen of NH_2 interacted with a lone pair of NH in MET769. The SAR study of these compounds is illustrated in Fig.7.

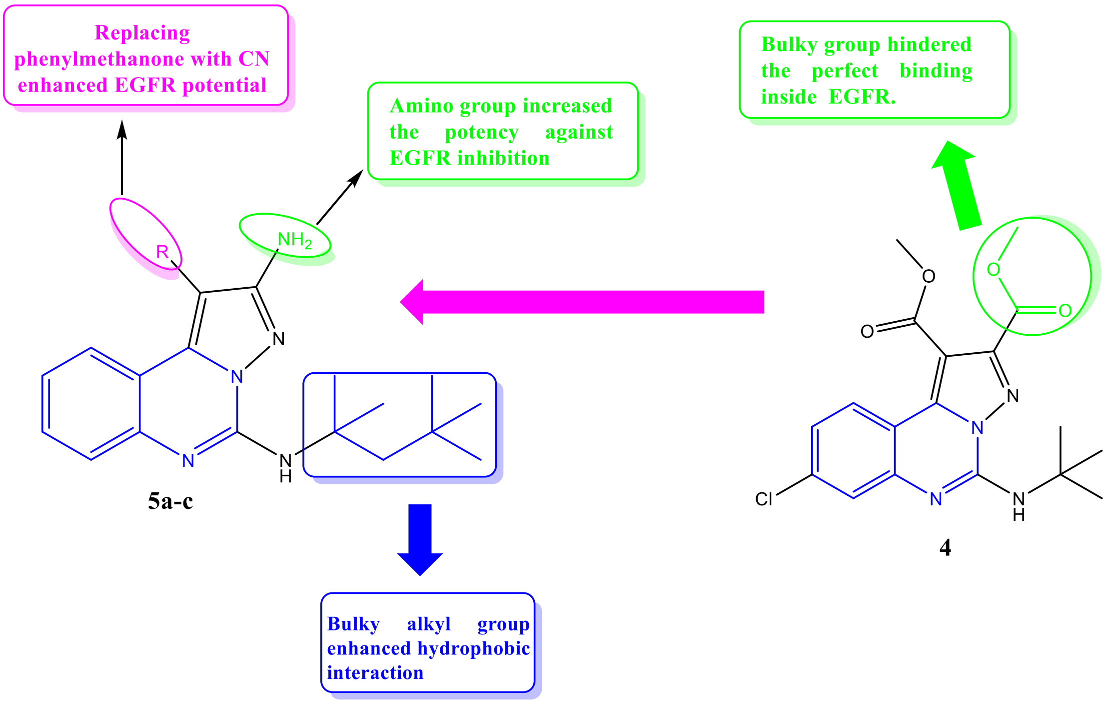

Fig.7. SAR and substitution effect on EGFR inhibition of compounds **4** and **5a-c.**

Table 1. Cytotoxicity and EGFR inhibition of **5a-c**, Erlotinib and Gefitinib.

Compound	R	MDA-MB-231 IC_{50} (µM)	A549 IC_{50} (µM)	H1299 IC_{50} (µM)	EGFR inhibition IC_{50} (nM)
5a	CN	1.96±0.23	2.87±0.29	2.02±0.34	165.38±0.29
5b	CO(4-F-C_6H_4)	1.93±0.55	1.06±0.48	1.32±0.56	157.63±0.34
5c	CO(4-OCH_3-C_6H_4)	2.45±0.31	1.74±0.23	2.04±0.33	216.35±0.22
Gefitinib	--------------	6.85±0.18	2.65±2.65	3.02±0.29	--------------------
Erlotinib	---------------	4.56±0.46	2.98±0.39	3.33±0.31	201.34±0.39

In Fig. 8, the binding free energies (ΔG) for the anticancer drugs Gefitinib (**1**) and Erlotinib (**2**) were compared to compounds **3**, **5a**, and **5b** as ligands docked at EGFR kinase (PDB ID: 1M17) and COX enzyme (PDB ID: 1CX2) receptors. The best poses obtained in the molecular-docking analyses were revealed. A lower ΔG indicates a more significant interaction between the receptor and the ligands with potential activity. Compound **3** displayed higher binding affinities than **5a**, **5b**, and controls at both receptors with high docking scores: -9.8 kcal/mol at 1M17 and -11.0 kcal/mol at 1CX2.

The 4-fluorophenyl moiety of **3** appeared to be responsible for the higher binding free energies, which aligns with the cytotoxic and protein kinase inhibition on EGFR and COX-2 activities.

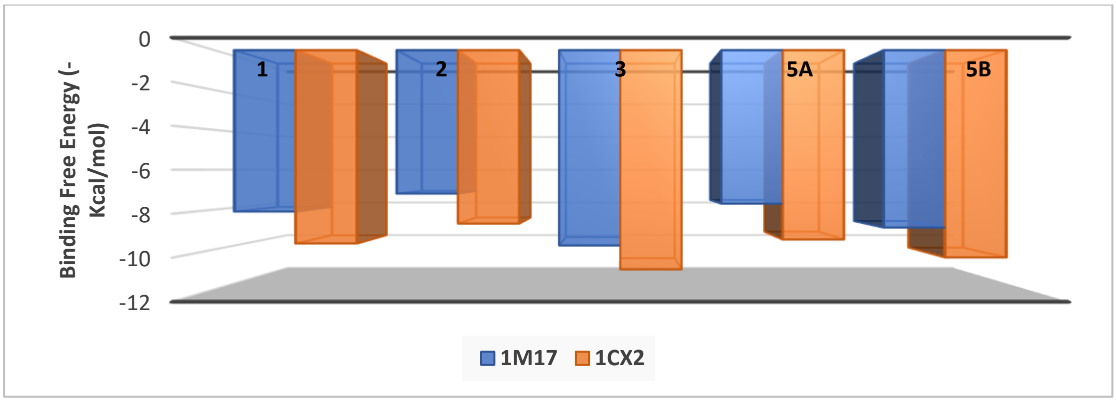

Fig. 8. Binding free energy values have been calculated for compounds **3**, **5a**, and **5b** in comparison to controls **1** and **2**. These compounds were utilized as ligands with 1M17 and 1CX2 receptors during molecular docking.

Figures 9A and 9B illustrate the docking details of compound **3** towards 1M17 and 1CX2 receptors, respectively. The conventional hydrogen bonding interaction between ASP A:813, ARG A:817, ASN A:818, and GLY A:833, and compound **3**'s high binding affinity with 1M17 (-9.8 kcal/mol) contribute to the strong receptor-ligand binding. Additionally, π -anion, alkyl, π -cation, and π -alkyl hydrophobic interactions were also observed with ASP A:831, ILE A:735, ARG A:817, ALA A:719, LEU 820, and VAL A:702 moieties of 1M17. The salt bridge formed between a positively charged nitrogen and a negatively charged oxygen was determined with GLU A:738. However, unfavorable donor-donor interaction was identified between compound **3** and LYS A:721, which may cause instability of the protein-ligand complex due to the repulsion between the two molecules or atoms (Figure 9A).

It was observed that compound **3** had more interactions with the 1CX2 residues than 1M17 moieties, which explains the binding affinity (-11.0 kcal/mol). Conventional hydrogen bonds and carbon-hydrogen interactions were noticed with moieties such as ARG A:469, SER A:471, TYR A:122, CYS A:47, GLN A:42, ASN A:39, and ASN 43 (Figure 9B). Other hydrophobic interactions, such as π -σ with LEU A:152, π -alkyl with PRO A:153, CYS A:36, CYS A:47, ARG A:44, ARG A:469, and LYS A:468, were also noticed. Additionally, halogen (fluorine) interaction between **3** and CYS A:47 was indicated in the presence of unfavorable donor-donor affinity with SER A:471.

Protein-ligand interactions are predominantly dominated by hydrophobic contacts. This category of interactions is largely produced by an aliphatic carbon in the receptor and an aromatic carbon in the ligand, indicating that small molecule inhibitors frequently contain aromatic rings. The most common aromatic ring found is the benzene ring system, which is present in 76% of commercially available medications. While π-cation interactions in protein structures have been extensively researched, the second most frequent hydrophobic connections occur between an aromatic or aliphatic carbon from the ligand and a chlorine or fluorine atom from the protein. Salt bridge interactions occur twice as frequently with positive nitrogen from the protein and negative oxygen from the ligand, compared to the opposite arrangement. The strength of salt bridge interactions is significantly influenced by the environment, with buried salt bridges contributing to ligand binding [62].

A

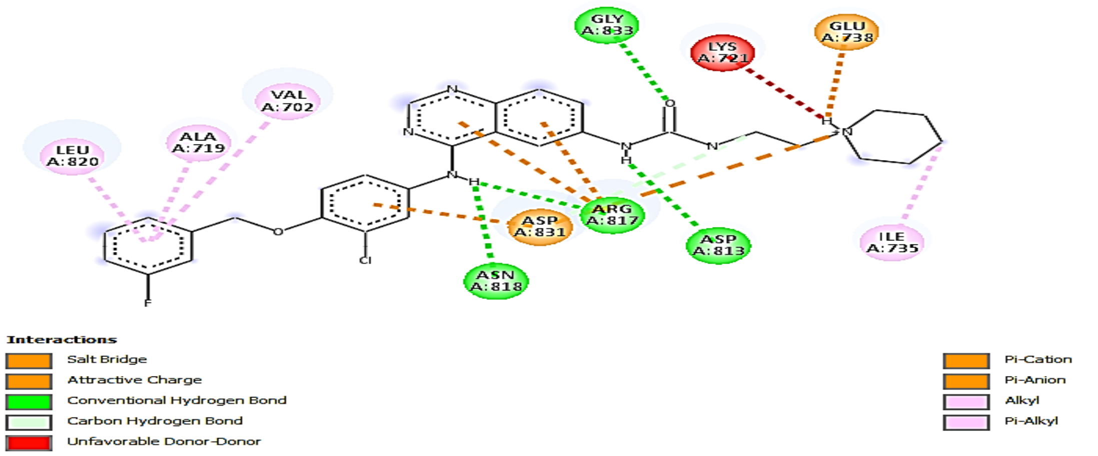

B

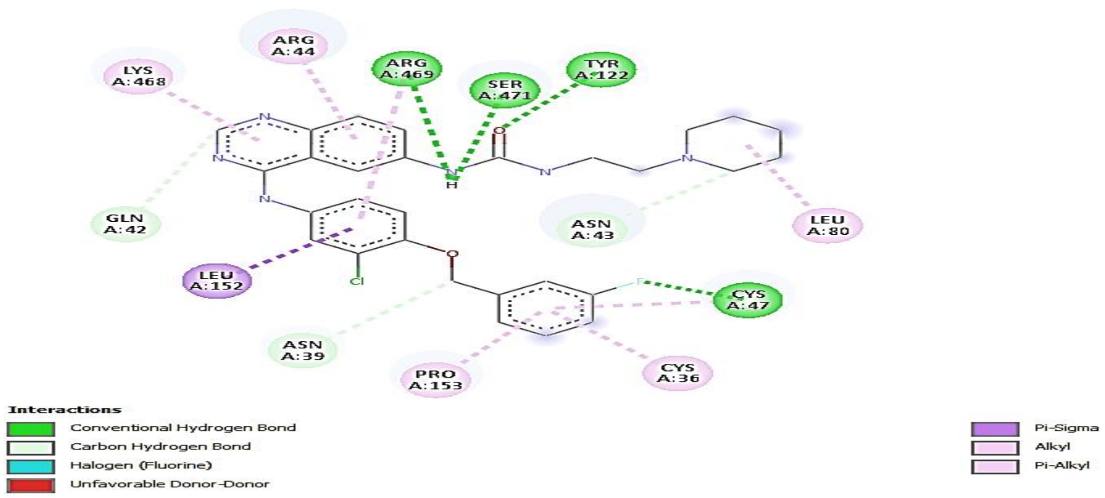

Fig. 9. In-silico figures illustrate the interactions between the compound **3** and (A) 1M17 and (B) 1CX2

In 2019, a new set of new thiophene having quinazolines was synthesized by Zou *et al*[63]. In this study, two modifications were performed on the chemical structure of Erlotinib**2**. The first modification was adding different alkoxy residues at C-6 and C-7 of Erlotinib to avoid covalent bond formation with Cys797 in EGFR that occurs in Erlotinib and causes dose-limiting toxicity. The second modification was introducing a rotatable C-N linkage between thequinazoline ring and thiophene moiety to improve conformational flexibility as revealed in Fig. 10.

These candidates were screened for their antiproliferative effect against A431 cell lines and for EGFR inhibitory potential. Compound **6** (Fig. 10) displayed anticancer activity with IC_{50} = 3.4 μM against the A431 cell line. Moreover, this thiophenoquinazoline derivative recorded EGFR inhibitory potential with IC_{50} = 4 μM. SAR displayed that the existence of electron-withdrawing groups on the thiophene moiety at C-5 markedly enhanced theEGFR inhibitory effect, and substitution at C-6 and C-7 of quinazoline increased EGFR inhibitory potential.

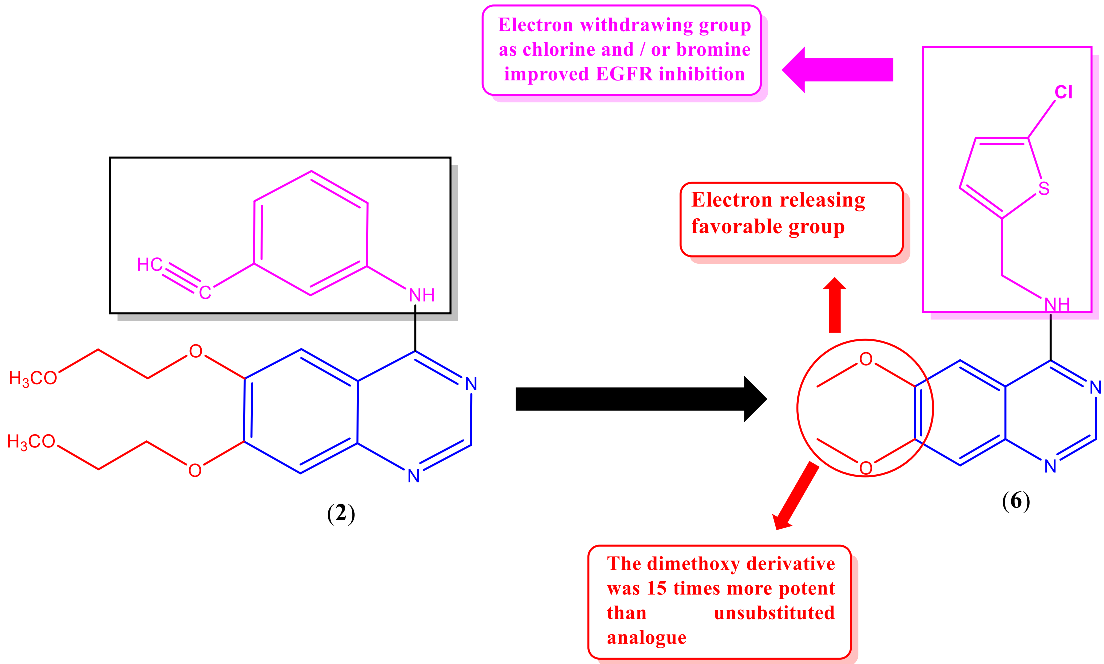

Fig.10. Design, Chemical structure and, SAR of quinazoline derivative **6**.

A novel set of quinazoline derivatives substituted with benzamide moiety at C-6 was identified as antiproliferative agents with EGFR inhibitory activity [64]. Compound **7** (Fig. 11) having electron withdrawing groups at C-2 and C-5 of the benzamide moiety recorded excellent antiproliferative potential towards the H1975 cell line with IC_{50} = 5340 nM compared to Gefitinib (IC_{50} = 7184 nM). Furthermore, this compound was reported to be the most potent compound exhibiting an IC_{50} of 5 nM against the wild-type EGFR and 2.7 nM against EGFRd746-750. SAR study is illustrated in Fig. 11 showing the effect of substitution on the anilino moiety, replacing the chlorine atom with the fluoro atom decreased the potency by 10 folds. Moreover, the introduction of a cyano group to the *para*-position of aniline resulted in a dramatic drop (at least 485-fold) in potency.

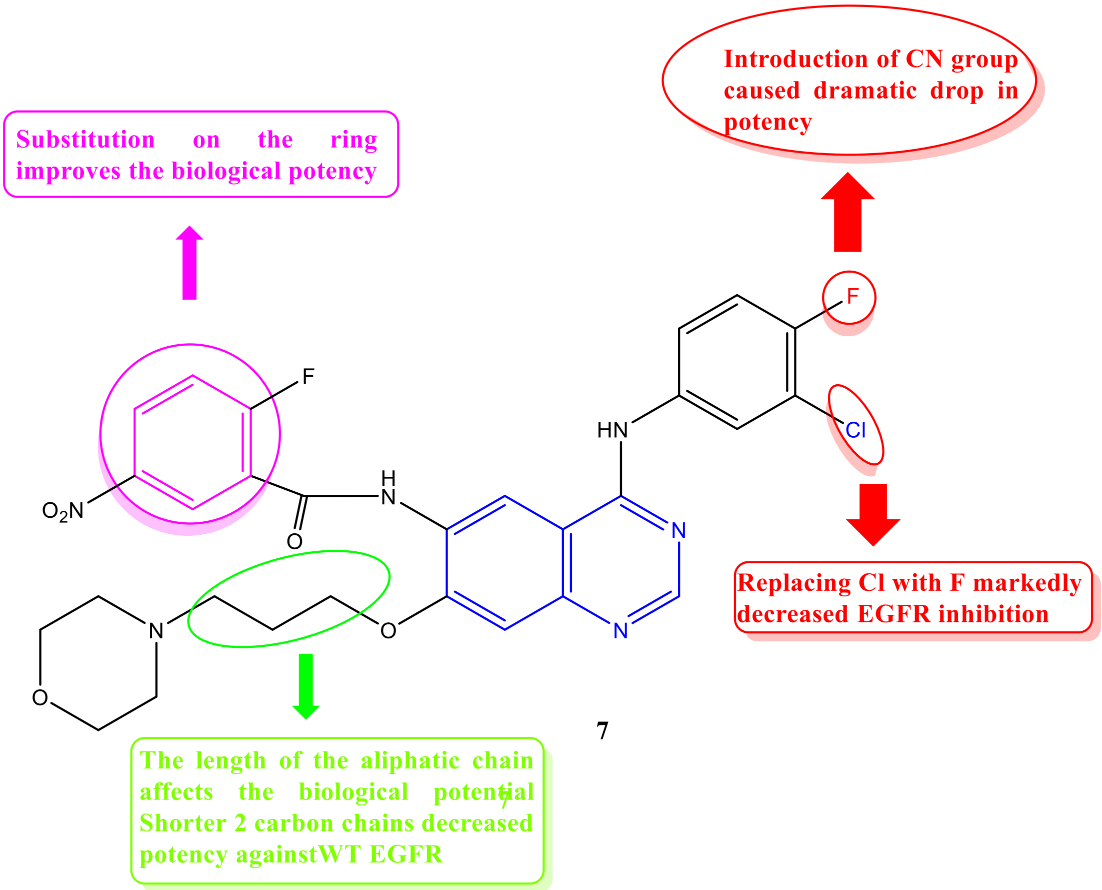

7

Fig. 11. Chemical structures of quinazoline derivative **7**.

Novel series of thiazolidinoquinazolin-4-one derivatives were synthesized and assessed for their antitumor activity toward HepG-2 and MCF-7 cell lines [65]. Design of the novel compounds based upon hybrid synthesis rather than one active pharmacophore. They hybridized quinazoline with thiazolidinone to affect hepatic cancer cells and breast cancer. From the target compounds, compound **8a** was the most active compound towards the hepatocellular cancer cell line (IC_{50} = 1.79 µM), while **8b** was the most potent against the breast cancer cell line (IC_{50} = 1.94 µM) (Fig. 12). A docking study of these compounds displayed excellent fitting within topoisomerase-II active site. SAR study revealed that the position and electronegativity of the substituent on the phenyl ring have a vital role in the anticancer activity of the synthesized compounds as shown in Fig 12.

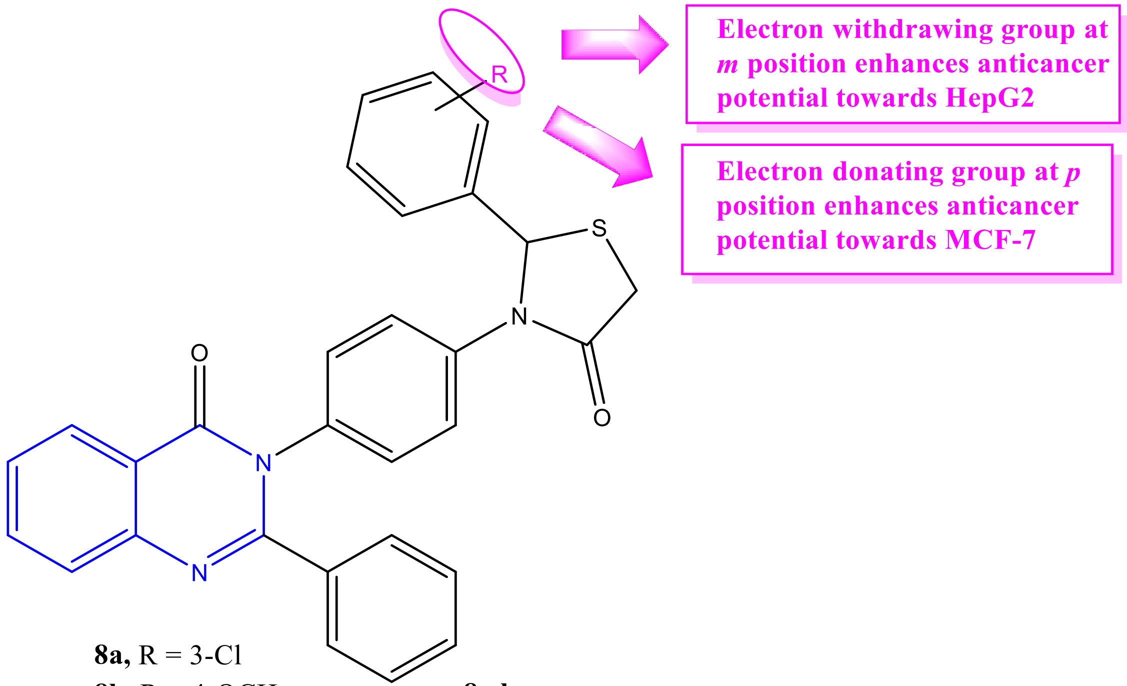

8a, R = 3-Cl
8b, R = 4-OCH_3

8a,b

Fig.12. The effect of electron donating and electron-withdrawing substituents on quinazolinones **8a,b.**

When tested against topoisomerase II (PDB IDs: 3QX3, 1ZXM, and 1RR8), both **8a** and **8b** showed similar binding capacities towards 3QX3 with an affinity of -8.8 kcal/mol. However, **8a** exhibited higher affinities towards 1ZXM (-9.6 kcal/mol) and 1RR8 (-9.3 kcal/mol) compared to **8b**.

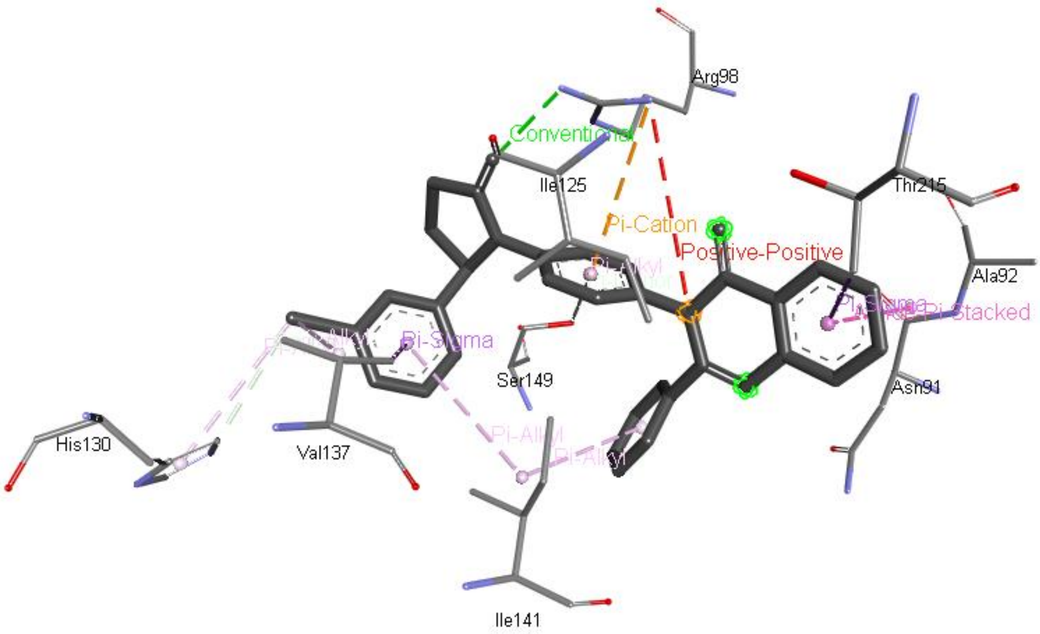

Fig. 13. Interaction of **8a** with topoisomerases II (1ZXM)

The higher binding affinity of **8a** on 1ZXM is attributed to the crucial conventional hydrogen, carbon-hydrogen, van der Waals, and π -donor hydrogen bonds formed with ARG A:98, HIS A:130, ALA A:92, and SER A:149 (Fig. 13). Alkyl interaction and π -alkyl bonds are common between **8a** and 1ZXM moieties, especially ILE A:125, ILE A:141, VAL A:137, and HIS A:130. In the same context, the strong π-σ bonds with VAL A:137 and THR A:215, in addition to the hydrophobic amide π-stacked bonding with ASN A:91, were also responsible for the higher affinity of **8a** toward 1ZXM (Fig. 13).

A new set of quinazolines having rhodanines was synthesized and screened for their cytotoxic potential against the human fibrosarcoma cell line (HT-1080) in 2017 [66]. All of the tested compounds revealed antiproliferative potential with IC_{50} = 10-60 µM. From inspecting the anticancer results, it is clear that the presence of hydrophobic, bulky and electron withdrawing moieties at the *para* position of the quinazolinone 3-phenyl ring as shown in compounds **9a-d** was essential for their anticancer activity

(Table 2, Fig. 14). The most active anticancer candidates were further tested towards two human leukemia cell lines, HL-60 and K-562, and the results are summarized in Table 2.

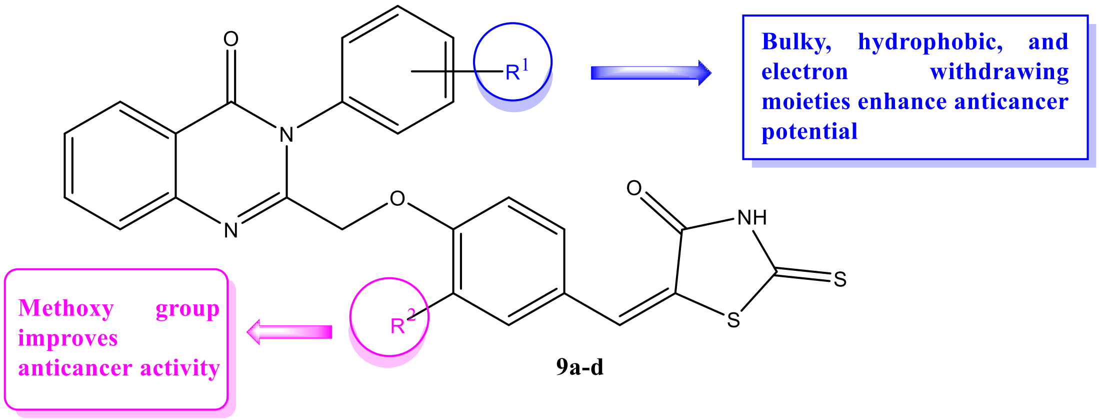

Fig. 14.SAR study of compounds **9a-d** as anticancer agents.

Table 2. IC_{50} (µM) for quinazoline derivatives **9a-d** against HT-1080, HL-60 and K-562 cell lines

Compounds	R^1	R^2	HT-1080	HL-60	K-562
9a	4-CF_3	H	15.8	5.5	5.0
9b	4-Cl	OCH_3	10.2	5.1	4.5
9c	4-Br	OCH_3	8.7	1.2	1.5
9d	4-CF_3	OCH_3	15.8	2.6	5.1

Novel quinazoline derivatives hybridized with triazole moiety were synthesized and screened for their antiproliferative potential against epidermoid carcinoma (KB), hepatoma carcinoma (HepG2) and lung cancer (SK-Lu-1)[67]. The rationale of this work is based upon introducing 1,2,3-triazolyl moiety on deoxygenated fused quinazolines at the anilino side chain suggesting that the triazole moiety would form extra H- bonds with the binding pocket of EGFR enzyme. All the assessed compounds displayed excellent cytotoxic activity especially **10** (Fig. 15) which was the most active antiproliferative agent with IC_{50} = 0.04, 0.14 and 1.03 µM against KB, HepG2 and Lu, respectively, in comparison with Erlotinib which had IC_{50} = 13.01, 25.01 and 99.76 µM, respectively.

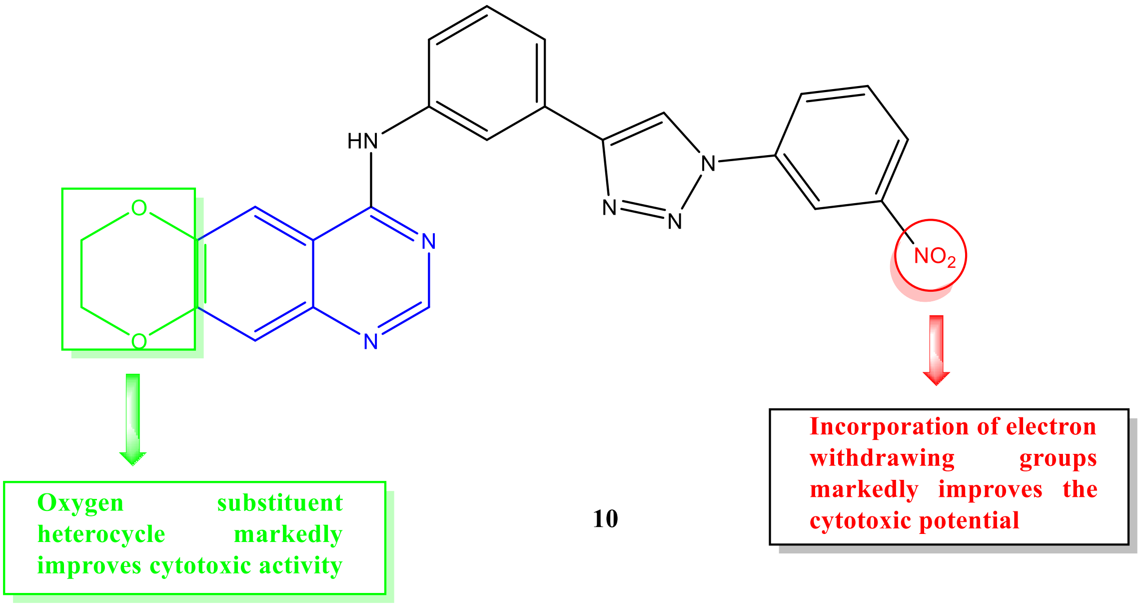

10

Fig. 15.SAR of quinazoline derivatives incorporating a triazole moiety **10** as anticancer agent.

Summary of the SAR of Quinazoline derivatives as anticancer agents:

SAR analysis of the anticancer potential of quinazolines showed some features as explained in Fig. 16.Nature of **s**ubstituents such as C-4, C-6 and C-7 has a significant effect on the antiproliferative activity of the quinazoline ring. The 4-Anilino ring is essential for the anticancer activity and lipophilic; electron-withdrawing substituents (Cl, Br) at meta position are optimal for activity. C-6 and, C-7 position side chains are primarily affecting their physicochemical properties allowing for good compatibility with bulky moieties. Electron-releasing groups at C-6 and, C-7 of quinazoline ring improve the anticancer potential.

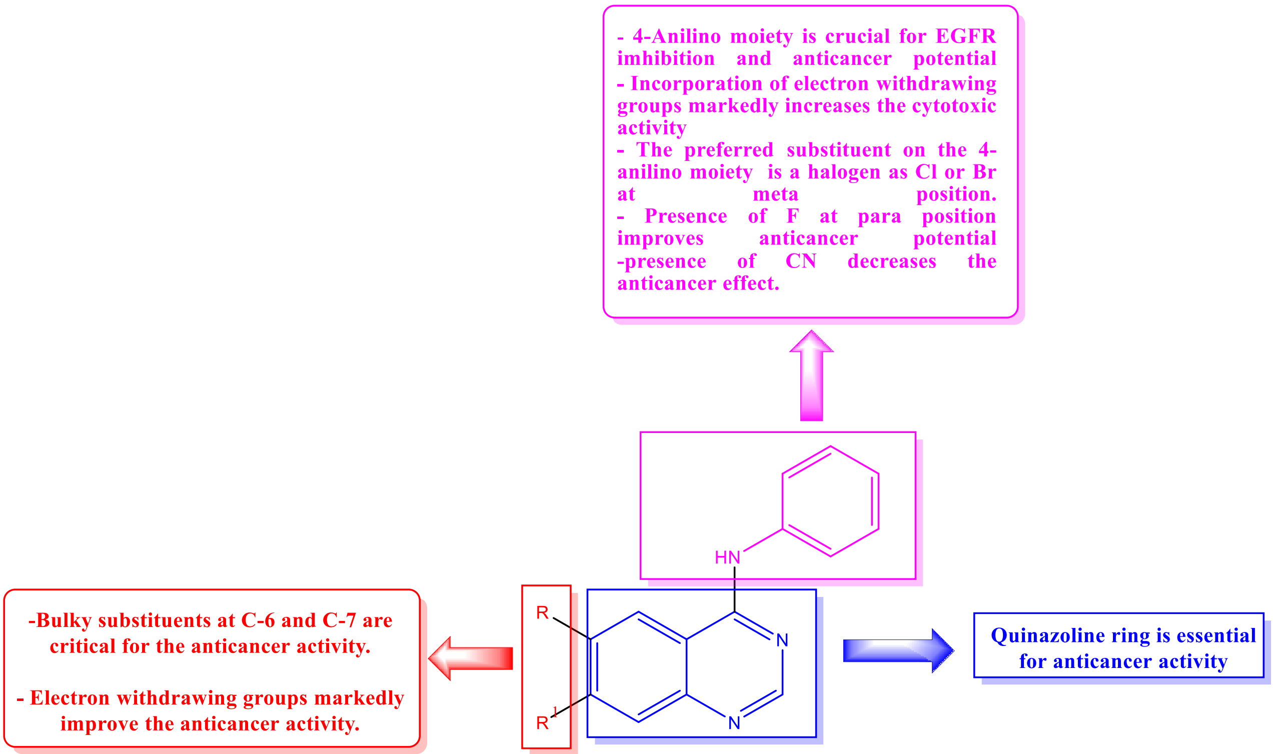

Fig. 16.SAR analysis of quinazolines as anticancer agents.

3.2. Anti-inflammatory activity

In 2015, novel derivatives of 4-aminoquinazolines were synthesized and tested for their anti-inflammatory potential [68]. Compounds **11a-d** were shown to have great TNF-α and IL-6 inhibition potential. SAR study was concluded from anti-inflammatory screening which revealed the significance of incorporating a heterocyclic moiety at the 4-phenyl position as depicted in Fig. 17.

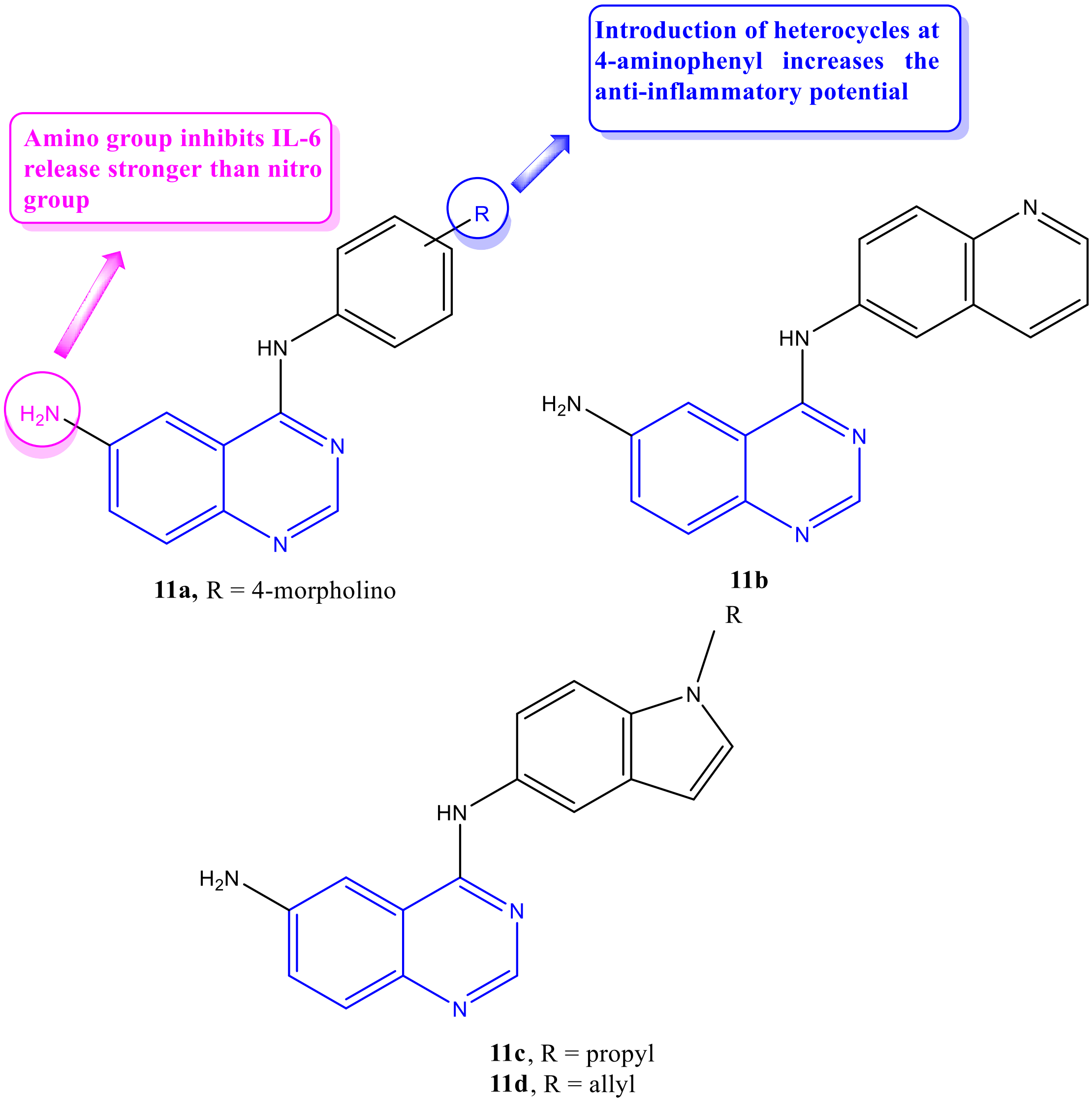

Fig. 17. SAR study of 4-aminoquinazolines as anti-inflammatory agents.

The binding free energies (ΔG) for the significant constituents of 4-amino quinazolines (**11a-d**) as ligands with TNF-α (PDB ID: 7JRA) and IL-6 (PDB ID: 1IL6) receptors are shown in Fig. 18, revealing the best poses obtained in the molecular docking analyses. Generally, **11a-d** displayed higher binding affinities at both receptors, with high docking scores of -6.3 to -7.0 kcal/mol at the 7JRA and from -7.4 to -7.7 kcal/mol at the 1IL6. Among the 4-amino quinazolines examined, **11b** and **11d** showed the highest binding affinity toward 7JRA (-7.0 kcal/mol), while **11b** had the highest bending energy toward 1IL6 (-7.7 kcal/mol).

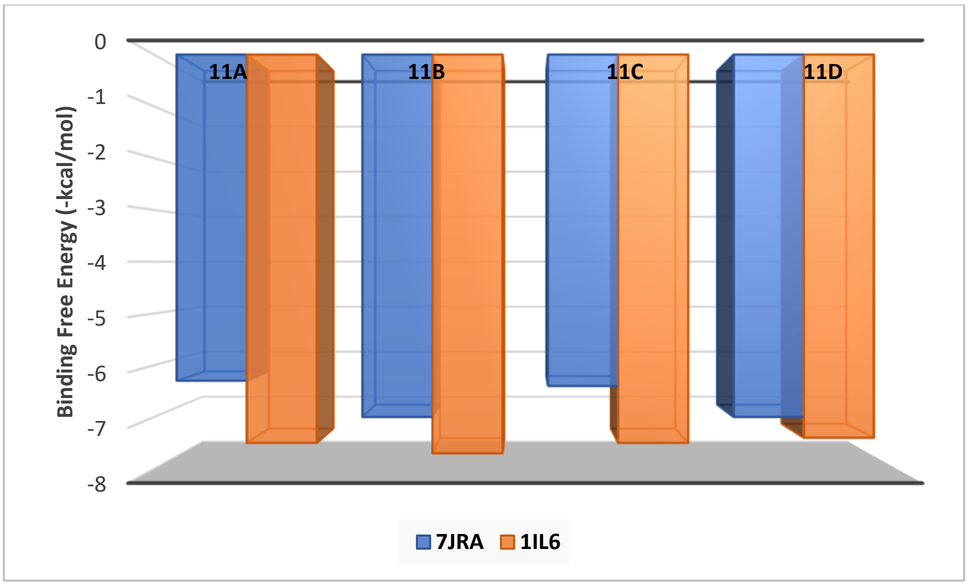

Fig. 18. Binding free energy values have been calculated for compounds **11a-d** ligands with 7JRA and 1IL6 receptors during molecular docking.

The higher binding affinity of **11b** with 1IL6 is attributed to the conventional hydrogen bonding with ARG A:169 and SER A:170. In addition, hydrophobic interactions between **11b** and the receptor moieties were observed; π –σ bond with LEU A:166, π-anion with GLU A:173, and π-alkyl interactions with LEU A:65, PRO A:66, MET A:68, and LEU A:166(Fig. 19). The types of interactions and the number of specific bonds were the main reasons for the differences in binding affinity between ligands against different receptors.

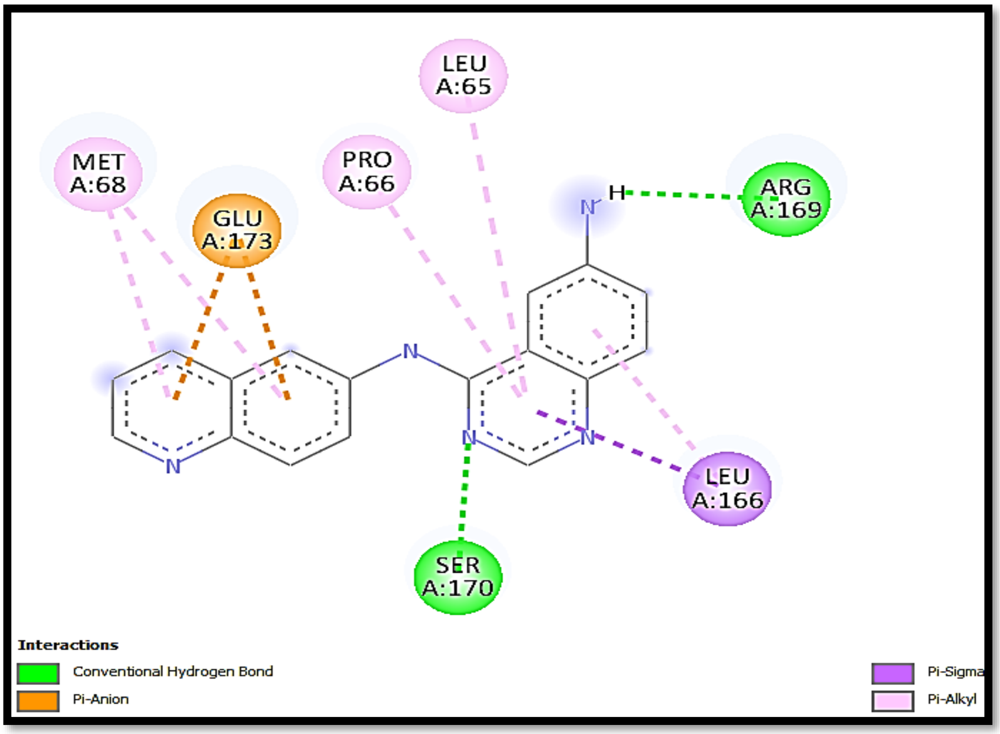

Fig. 19. The molecular interaction of **11b** with 1IL6 receptor.

A new set of quinazoline derivatives hybridized with isoxazole moiety was designed, synthesized and evaluated for their anti-inflammatory effect [69]. It was found that compounds having electron-withdrawing groups as compounds **12a,b** recorded higher anti-inflammatory potential than diclofenac as depicted in Table 3. In addition, substituent positions markedly influence the anti-inflammatory activity as compounds with *para* substitution revealed a higher anti-inflammatory effect than the *meta*-analogues (Fig. 20).

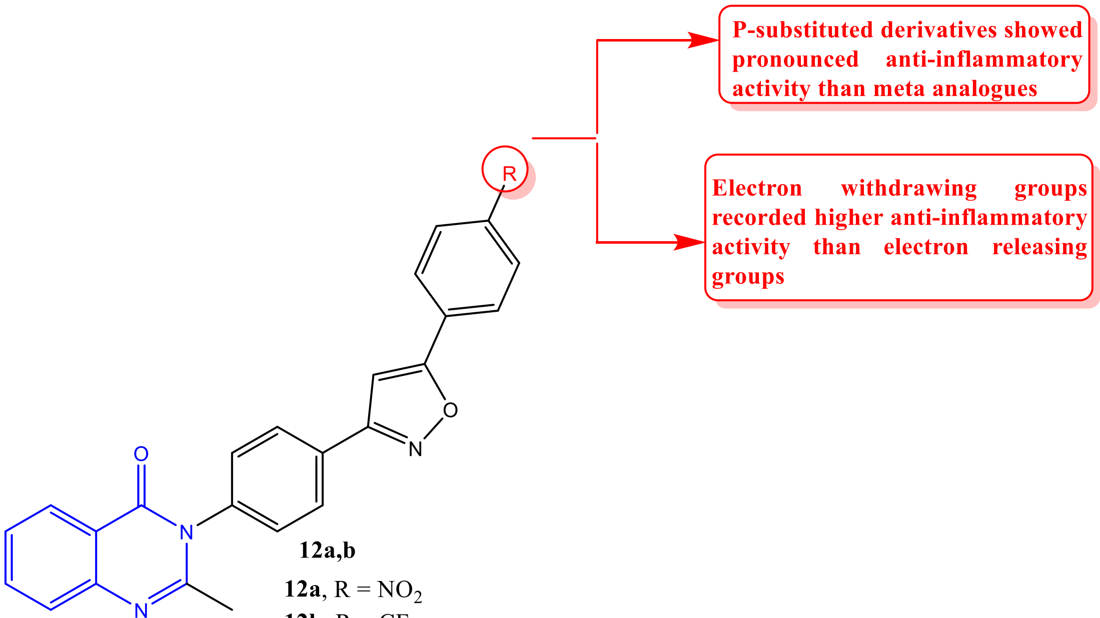

12a,b

12a, R = NO_2

12b, R = CF_3

Fig 20. Chemical structure of the anti-inflammatory quinazoline derivatives **12a,b**.

Table 3. Percent anti-inflammatory activity of the synthesized compounds **12a,b**

Compound number	Dose uM	30 Minutes	1 Hour	2 Hours	3 Hours
12a	10 20	34±0.51 48±1.06	41±1.85 56±0.53	45±2.06 64±1.92	38±0.67 50±1.60
12b	10 20	32±1.29 47±0.50	40±0.65 53±1.76	44±1.83 62±1.18	35±1.46 46±1.93
Diclofenac	10 20	29±0.46 42±1.63	37±1.19 51±1.36	42±0.71 60±0.81	33±1.53 44±1.55

A new set of 3-substituted-7-chloroquinazoline was synthesized and evaluated for their anti-inflammatory activity using a carrageenan-induced paw edema procedure in rats [70].The rationale of this work is based upon substitution at 2nd and 3rd position of quinazoline derivatives in an attempt to get more potent and selective anti-inflammatory agents. From the prepared quinazolines, compounds **13a-c** showed excellent anti-inflammatory activity as shown in Table 4. SAR study displayed that incorporation of amino, urea and/or thiourea at N-3 of the quinazoline scaffold was essential for the anti-inflammatory potential (Fig. 21).

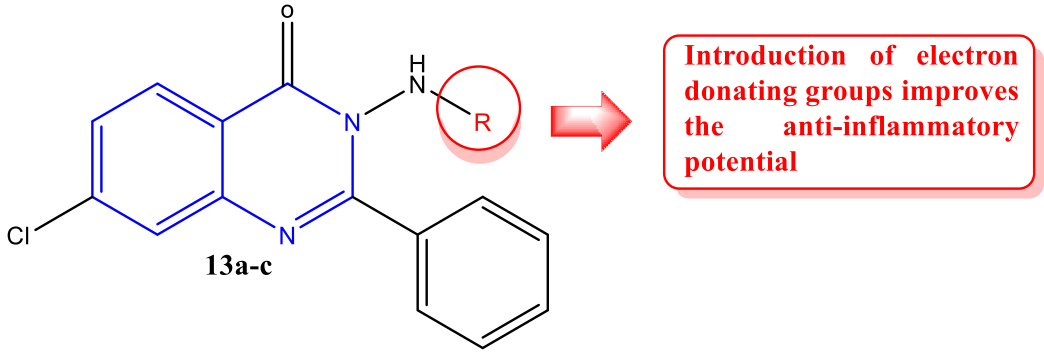

13a-c

Fig. 21. Chemical structure of the anti-inflammatory quinazolinone derivatives **13a-c**.

Table 4. Anti-inflammatory potential of quinazolines **13a-c**.

Compound number	**R**	**% Inhibition**
13a	NH_2	68.57
13b	$CONH_2$	62.85
13c	$CSNH_2$	65.71
Diclofenac	-----------------	71.42

Furthermore, 4,6-disubstituted quinazolines were prepared and tested for their anti-inflammatory activity by Chandrika *et al*[71]. Compound **14** (Fig. 22) having L-methylglycine at position 4 of the quinazoline ring recorded the highest anti-inflammatory potential with inflammation inhibition percent = 9.30% compared with the standard drug indomethacin which showed inflammation inhibition percent = 48%. Recently, in 2020, a new set of 2,3-disubstituted quinazoline-4-one derivatives was synthesized and evaluated for their anti-inflammatory activity [72]. Compounds **15a, and b** (Fig. 22) revealed anti-inflammatory potential *via* suppressing the release of inflammatory mediators such as histamine, serotonin and prostaglandin.

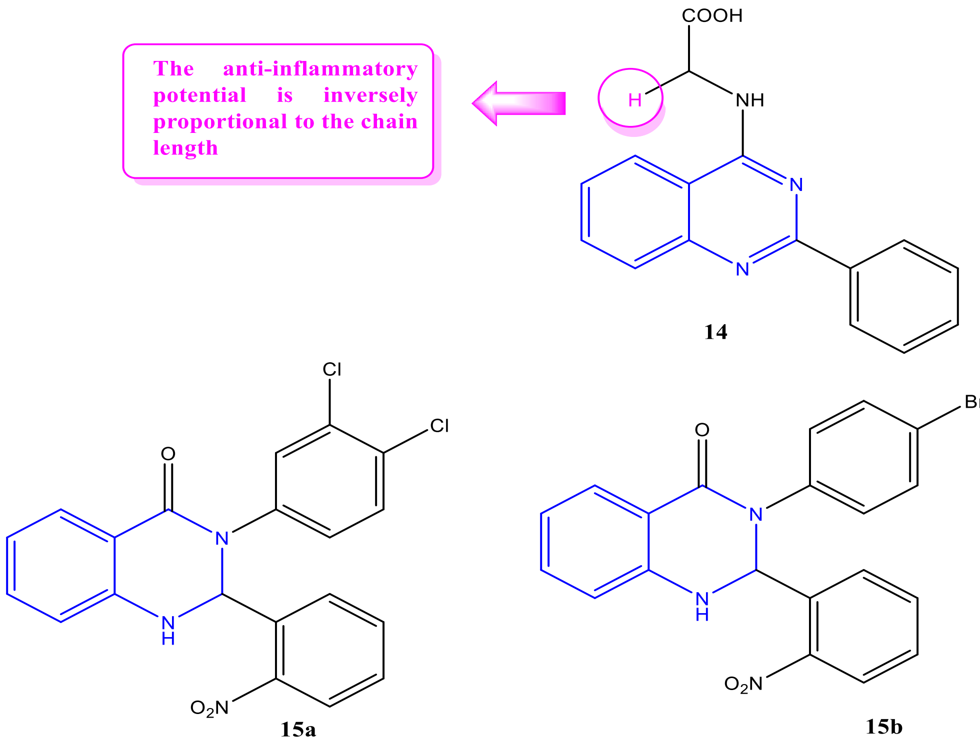

Fig. 22. Chemical structure of quinazoline derivatives **14** and**15a,b**.

Summary of the SAR of Quinazoline derivatives as anti-inflammatory agents:

SAR analysis of the anti-inflammatory activity of quinazoline derivatives displayed that substitution at C-2 and N-3 are significant for the anti-inflammatory activity. Moreover, the presence of an electron donating group at N-3 markedly increased the anti-inflammatory activity. In addition, molecular hybridization of 4-anilino moiety with another heterocycle markedly improved the anti-inflammatory effect as explained in Fig. 23.

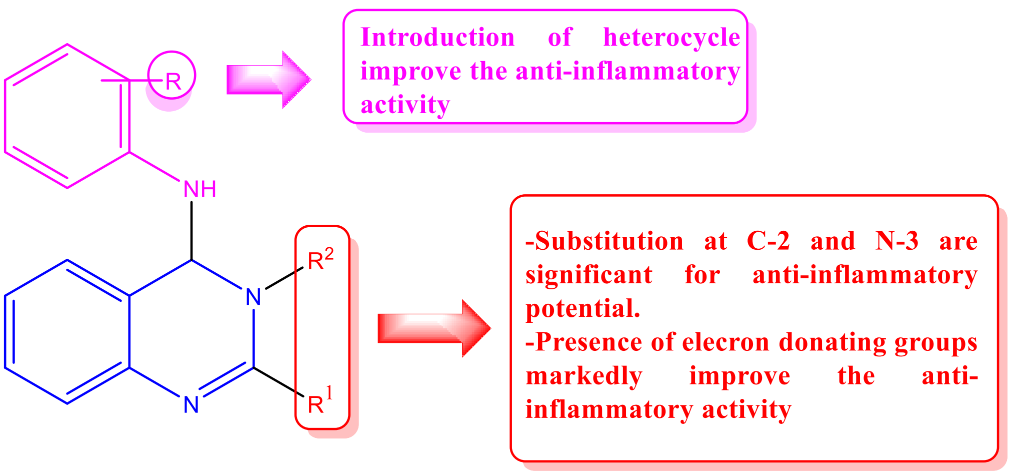

Fig. 23.SAR analysis of quinazolines as anti-inflammatory agents.

3.3.Antimicrobial activity

New derivatives 1-*N*-substituted-3-(4-(5-pyridin-3-yl)-1,3,4-oxadiazol-2-ylthio) quinazoline-6-yl)urea/thiourea (**16a-e**) and 1-*N*-substituted-3-(7-(4-methylpiperazin-1-yl)-4-(5-pyridin-3-yl)-1,3,4-oxadiazol-2-ylthio)quinazoline-6-yl) urea/thiourea (**17a-e**) were synthesized and assessed for their antimicrobial activity against *Bacillus subtilis*, *Staphylococcus aureus*, *Escherichia coli* and *Pseudomonas aeruginosa*[21]. From the antimicrobial outcomes, all the prepared compounds were found to exhibit broad-spectrum potential towards all the tested microbes with MIC range = 6.25-100 µg/ml. Compound **16a** recorded broad-spectrum antimicrobial activity towards all the screened species. SAR was conducted to get insights into the pharmacophoric moieties essential for the antimicrobial activity as depicted in Fig. 24& Table 5.

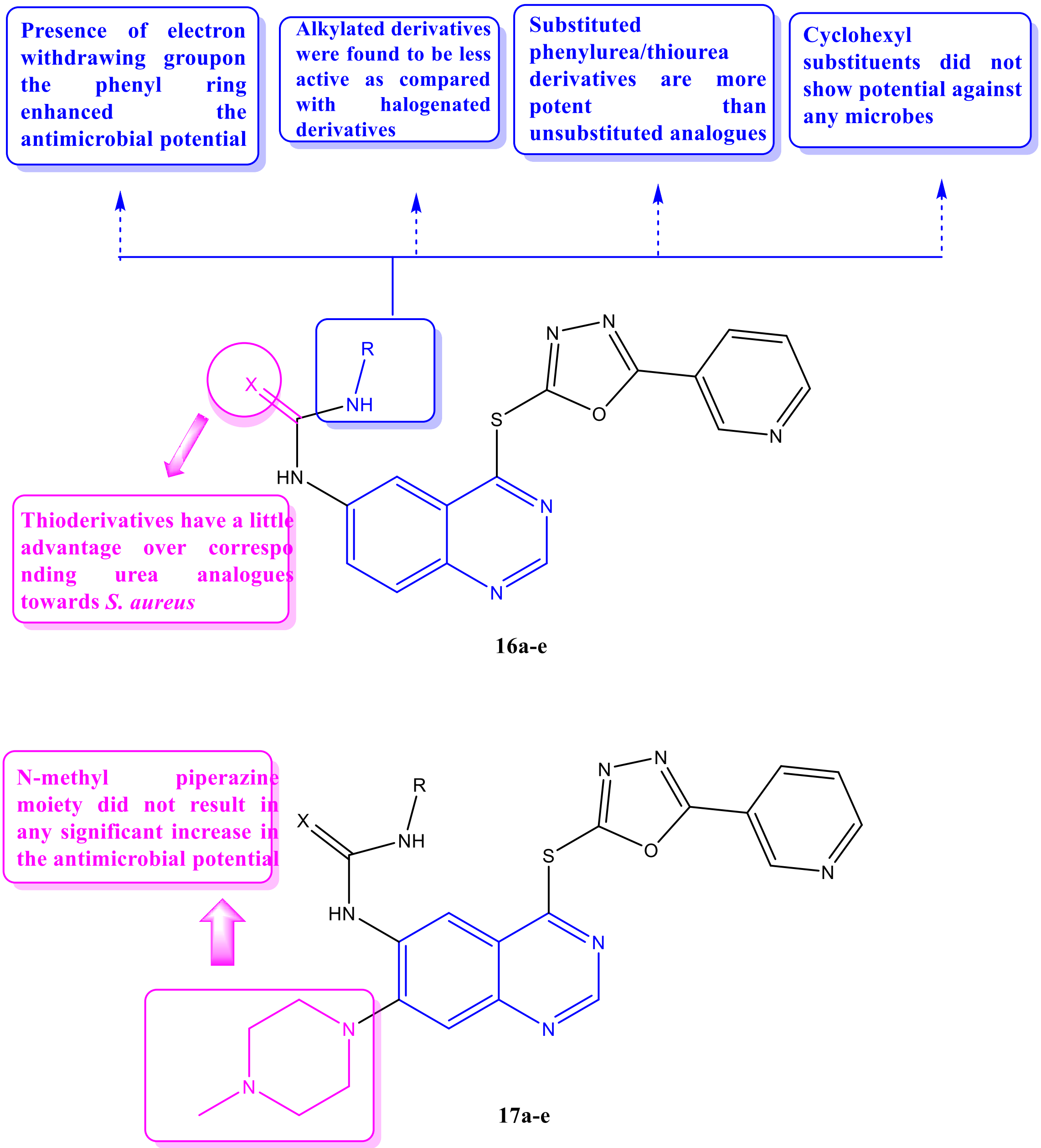

Fig. 24. SAR and substitution effect of quinazolines on the antimicrobial activity.

Table 5. Antimicrobial results (MIC in µg/ml) of compounds **16a-e** and**17a-e**

Compound number	R	X	*S. aureus*	*B. subtilis*	*P. aeruginosa*	*E. coli*
16a	3-CH_3-C_6H_4	O	25	25	50	12.5
16b	Cyclohexyl	O	25	50	100	50
16c	4-Cl-C_6H_4	O	6.25	25	75	50
16d	3-CH_3-C_6H_4	S	75	75	100	50
16e	4-F-C_6H_4	S	6.25	6.25	50	12.5
17a	3-CH_3-C_6H_4	O	50	25	50	25

17b	Cyclohexyl	O	50	12.5	50	25
17c	3-Cl-C_6H_4	S	6.25	25	50	12.5
17d	4-Cl-C_6H_4	S	25	12.5	50	50
17e	2-CH_3-C_6H_4	S	50	75	25	100

To better understand how compound **16e** provides antibacterial activity, a molecular-docking approach was used in silico. This compound showed a potential activity according to Table 5. Antibiotics work by deactivating vital enzymes involved in microbial metabolism, which restricts their growth and affects biosynthesis and repair of cell walls, proteins, and nucleic acids. Enzymes such as isoleucyl-tRNAsynthetase (PDB ID: 1JZQ), DNA gyrase (1KZN), dihydropteroate synthase (2VEG), D-alanine ligase (2ZDQ), topoisomerase 4 (3RAE), dihydrofolate reductase (3SRW), and penicillin-binding protein (3UDI) are targeted by antibiotics [73]. The best docking score was -12.3 kcal/mol towards 2ZDQ (Fig. 25); therefore, binding analysis was performed to reveal the interaction between the compound **16e** and 2ZDQ protein-binding sites (Fig. 26).

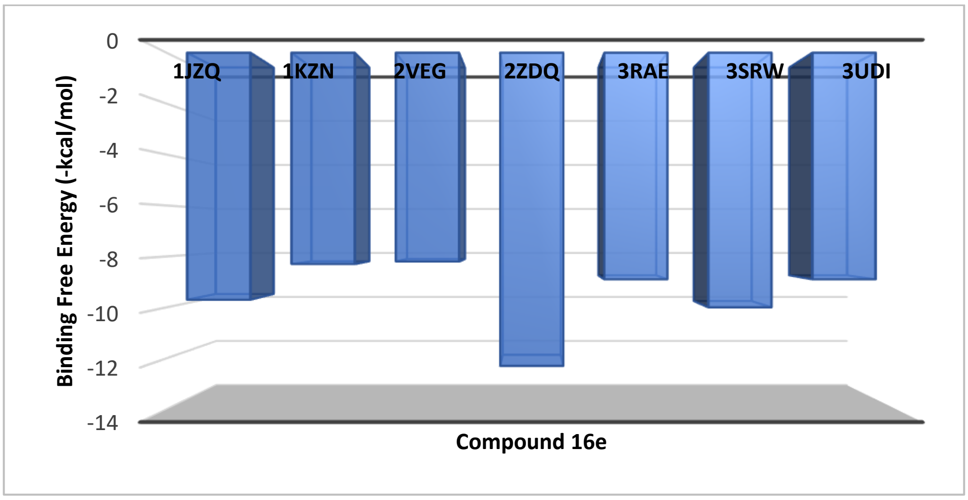

Fig. 25. Binding free-energy values calculated through the molecular docking of compound**16e** and the bacterial key metabolic enzymes as receptors.

Fig. 26 illustrates the docking details of compound **16e** towards 2ZDQ. The highest receptor-ligand binding position scores are due to the formation of conventional hydrogen bonding and carbon-hydrogen interaction with TYR A:218, MET A:294, THR A:292, TYR A:223, SER A:160, and PHE A:151. Additionally, hydrophobic interactions such as π- π stacked, π-alkyl, π-cation, π-anion, and π-sulfur, were observed with PHE A:151, PHE A:272, LYS A:228, LEU A:192, VAL A:195, ARG A:268, LYS A:228, ASP A:270, TYR 223, and MET A:294 moieties of 2ZDQ. In the study, it was noticed that halogen (fluorine) interactions of type C–X···Y (where X = F and Y = O, N, S) occurred between protein side chains or backbone (LYS A:190) and halogen atoms (XB donor) resulting in halogen bonding (XB) interactions (as shown in Figure **21**). The halogen atom's σ-hole (positive electrostatic potential) served as the XB donor and the XB acceptor was a nucleophile. According to [74], the second most common hydrophobic contacts observed were between an aliphatic or aromatic carbon in the protein and a chlorine or fluorine in the ligand. The interactions between the side chain sulfur atom of methionine and the ligand's aromatic carbon followed next.

The contact between a positively charged nitrogen coming from the protein and a negatively charged oxygen coming from the ligand (i.e. salt bridge) was also detected in Fig. 26 with GLU A:197.

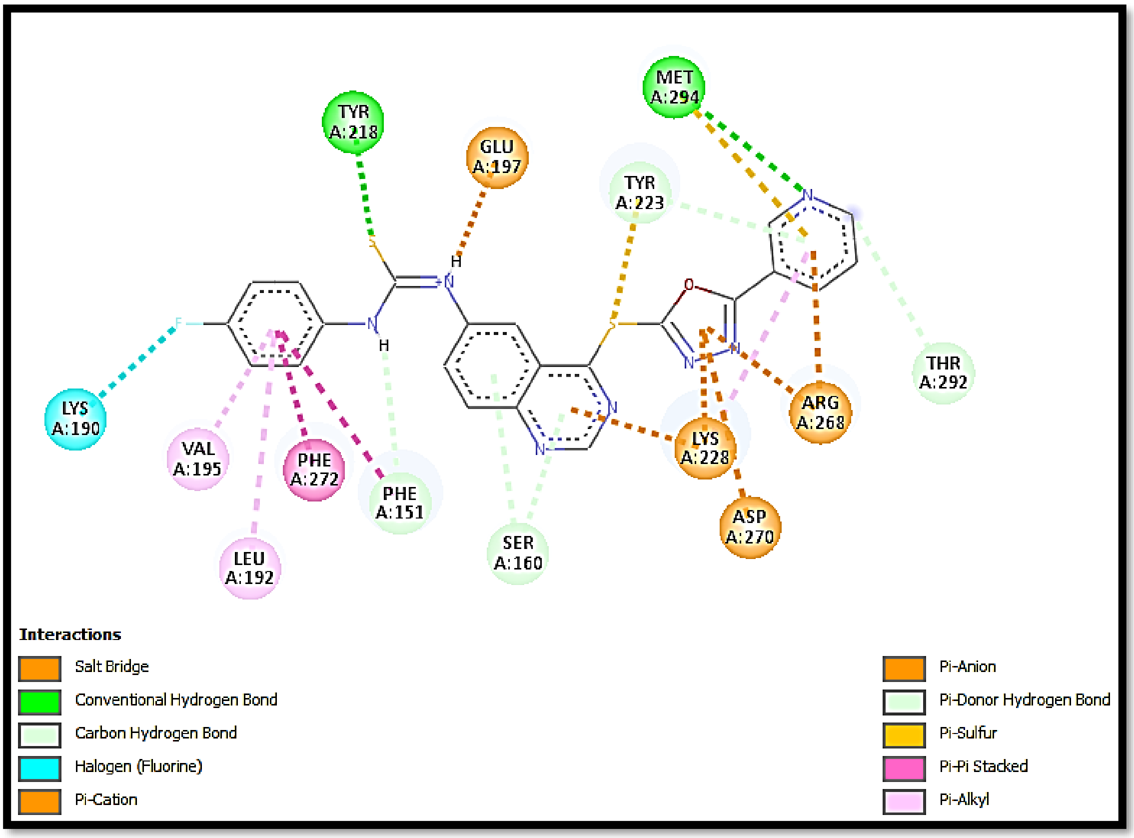

Fig. 26. Visualization for the docked compound **16e** and 2ZDQ

In 2021, novel quinazoline derivatives containing thiazolidine and pyridine moieties **18a-e** (Fig. 27) were synthesized and tested for their antibacterial and antifungal activity [75]. The authors designed the target compounds **18a-e** by conducting some modifications on the commercially used drugs rosiglitazone, fluquinconazole and albaconazole. Rosiglitazone has pyridine and thiazolidinedione heterocycles; the authors clubbed the pyridine and quinazoline with thiazolidin-4-one moiety. Fluquinconazole has quinazoline and 1,2,4-triazole moiety, the authors replaced the phenyl ring with thiazolidin-4-one and triazole with phenyl ring. Albaconazole contains quinazoline and 1,2,4-triazole moiety, they modified quinazoline on 2nd carbon with phenyl ring and added thiazolidin-4-one moiety as shown in Fig. 27.

In this study, it was found that compounds having electron donating groups at C-5 of thiazolidinone moiety exhibited prominent antibacterial potential such as **18a** (R = CH_3) and **18b** (R = $(OCH_3)_2$ (MIC = 62.5 µg/ml) compared to chloramphenicol (MIC = 50 µg/ml) against *P. aeruginosa*. On the other hand, compounds with electron-withdrawing groups displayed excellent antifungal activity. For example, **18c, 18d** and**18e** recorded similar antifungal activity against *A. niger* with MIC = 100 µg/ml.

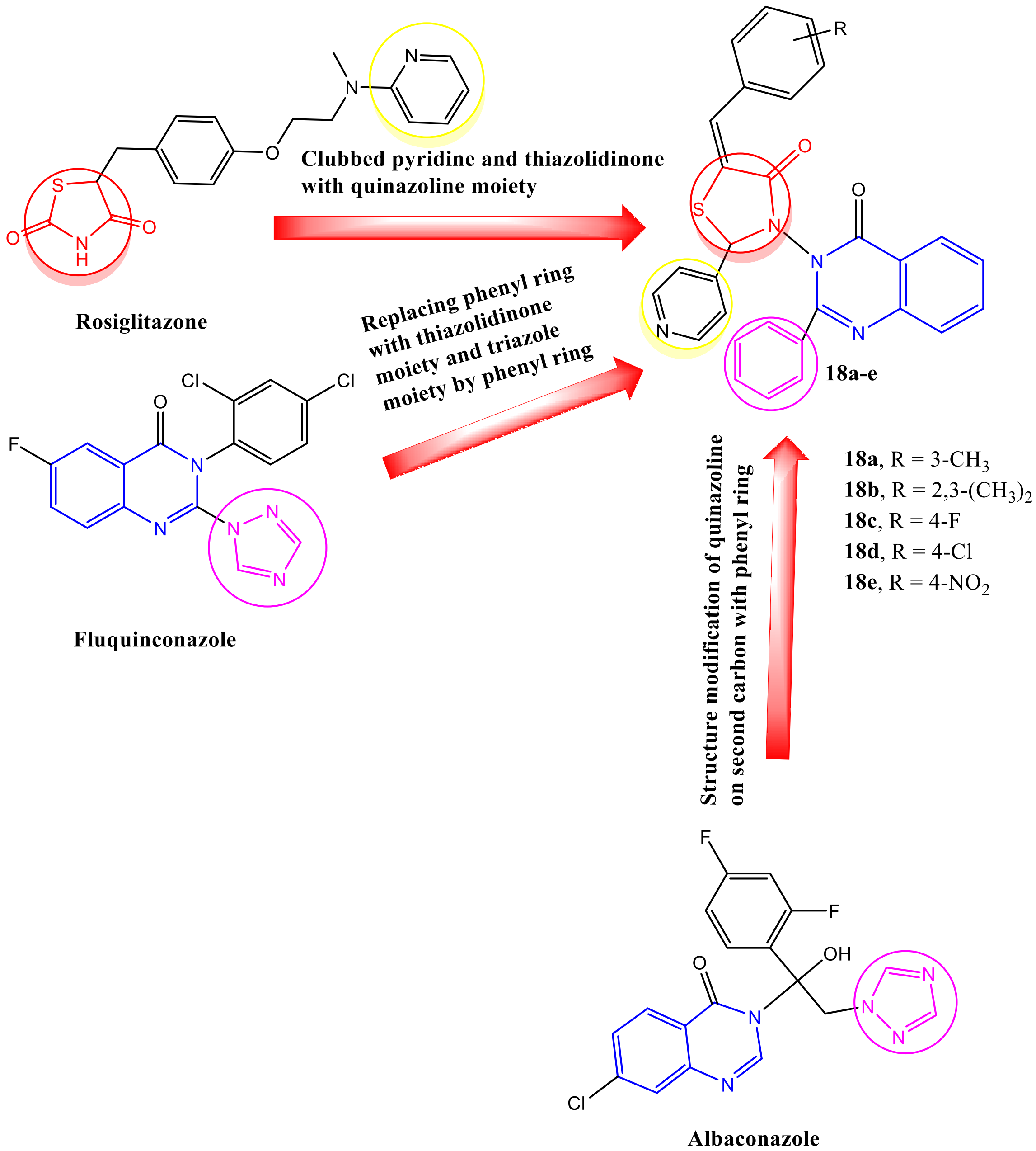

Fig. 27. Rationale design of quinazolinone derivatives **18a-e**as antimicrobial agents.

In silico study through molecular docking was conducted for the compound **18c** as an example of the most potent antifungal agent with polyketide synthase, cytochrome P450 monooxygenase, non-ribosomal peptide synthase, and halogenase enzymes which play a key role in AFB1 biosynthesis [76]. The highest binding affinities of **18c**were toward halogenase and cytochrome P450 monooxygenase; -9.8 kcal/mol for both enzymes, followed by -9.2 kcal/mol for both polyketide synthase and non-ribosomal peptide synthase enzymes.

A **B**

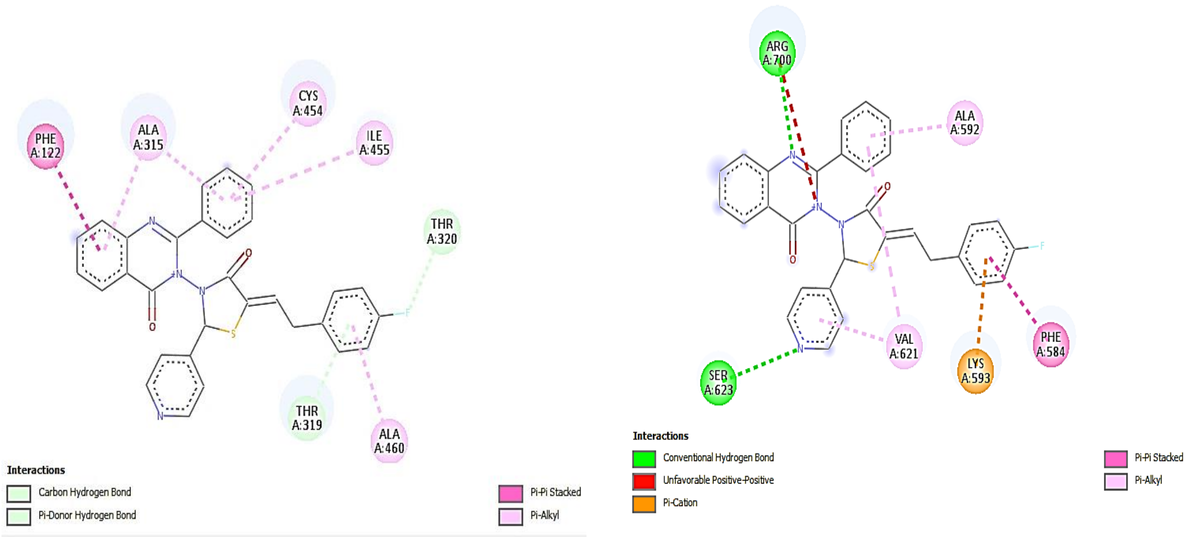

Fig. 28. The interactions of **18c** with cytochrome P450 monooxygenase (**A**) and non-ribosomal peptide synthase (**B**).

Based on the binding interaction analysis of the compound **18c** with both cytochrome P450 monooxygenase and non-ribosomal peptide synthase enzymes as examples for the higher and lower receptors according to the free binding energy, the same conventional, π-donor, and carbon-hydrogen bonds, in addition to hydrophobic interactions like π- π stacked, π-alkyl, and π-cation were detected between the ligand and both receptors (Fig. 28) However, the unfavorable positive-positive interaction between **18c** and ARG A:700 residue of non-ribosomal peptide synthase may be the main reason for the lower binding affinity due to its negative effect on the stability of the interaction (Fig. 28).

Moreover,2-(4-(2-(4-chlorophenyl)-4-oxoquinazolin-3(4*H*)-yl)phenoxy) acetohydrazide (**19**) (Fig. 29) was found to exhibit similar antibacterial activity (inhibition zone = 29 mm) as that of tetracycline (inhibition zone = 28 mm) against *Staphylococcus aureus*[77].

Furthermore, novel bis(azolylamino) **20-22** and bis(azolylmethylamino) **23-25** were synthesized and screened for their antimicrobial activity by Rekha *et al* [78]. From the antimicrobial results, it was found that quinazoline derivatives linked to an amino group at C-4 (compounds **20-22)** exhibited higher antimicrobial potential than analogues linked to a methylamino moiety **23-25**(Fig. 29).

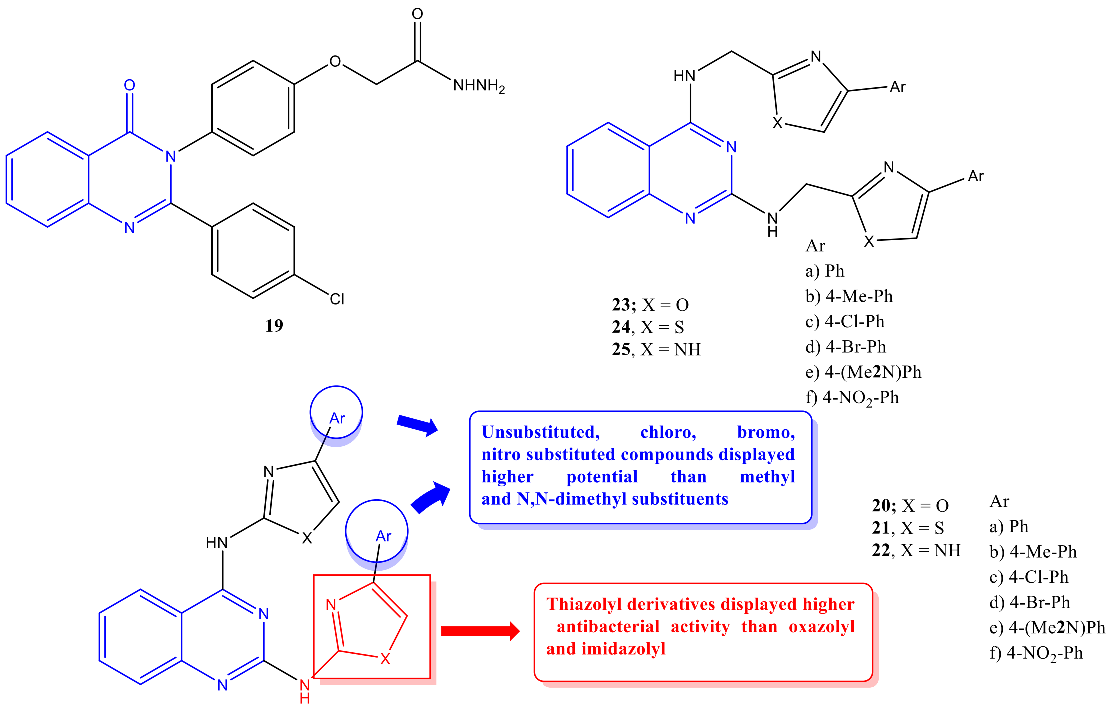

Fig. 29. Chemical structures of quinazoline derivatives**19-25.**

Summary of the SAR of Quinazoline derivatives as antimicrobial agents:

SAR analysis of quinazoline rings as antimicrobial agents showed that substitution at C-2 and N-3 improved the antimicrobial activity. The existence of asubstituted aromatic ring at N-3 is critical for the antimicrobial effect. Moreover, substitution at C-4 (mainly amine or substituted amine) enhances the antimicrobial potential.

3.4. Antidiabetic activity

In 2015, Gurram*et al*[79]synthesized novel 4,6-disubstituted quinazoline derivatives and screened them for their potential against *α*-glucosidase. Compounds **26a-g** exhibited excellent *α*-glucosidase inhibition (IC_{50} = 3.20-11.71 μM) compared to the standard drug acarbose (IC_{50} = 6.20 μM) Table 6. Moreover, it was found that substituting the amino group at C4 resulted in higher *α*-glucosidase inhibition compared to the unsubstituted analogues (Fig. 30).

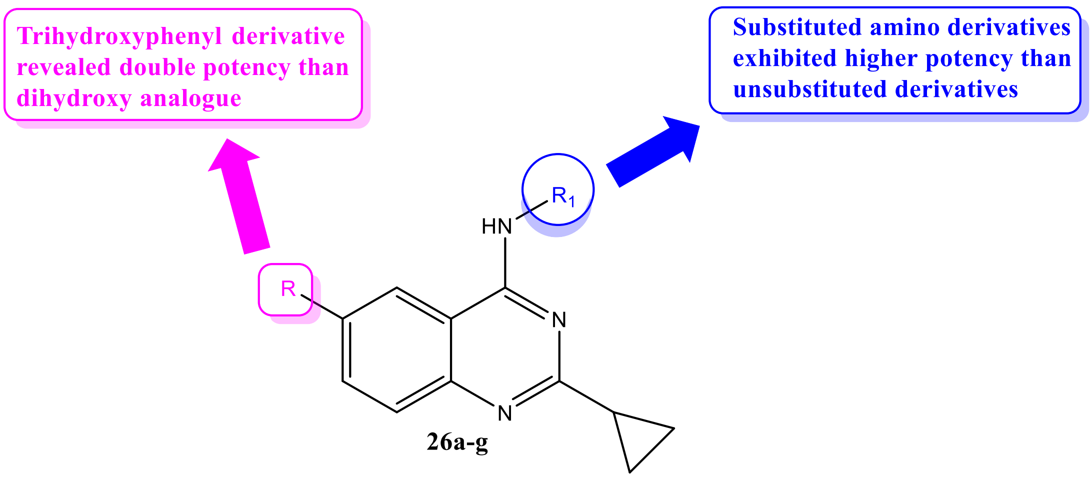

Fig. 30.SAR study for 4-aminoquinazoline derivatives**26a-g** as *α*-glucosidase inhibitors.

Table 6.IC_{50} of quinazoline derivatives **26a-g**as *α*-glucosidase inhibitors.

Compound number	Compound structure	α-Glucosidase inhibition (IC_{50}, μM)
26a	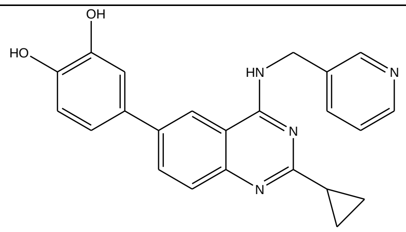	8.60

26b	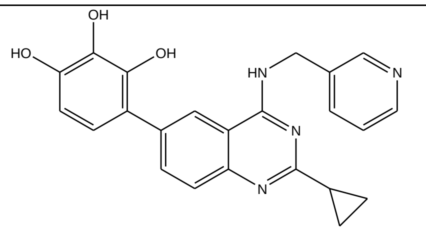	3.20
26c	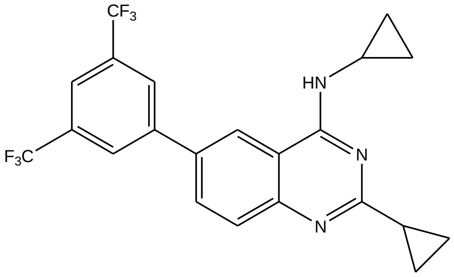	7.10
26d	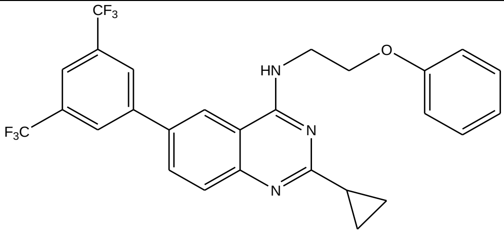	4.97
26e	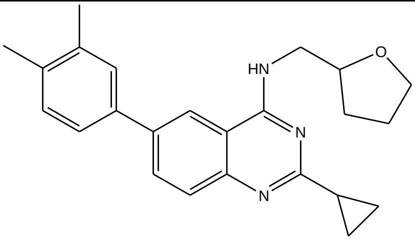	4.15
26f	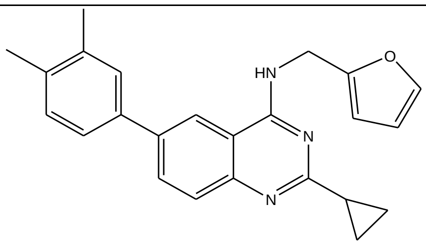	6.19
26g	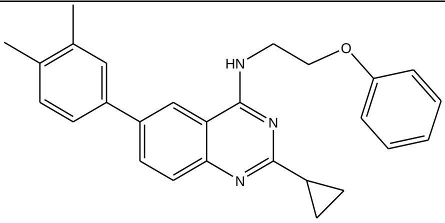	11.71
Acarbose	--------------------------------	6.20

Furthermore, compounds **27a,b** (IC_{50} = 2.6 and 2.96 μM) recorded higher α-glucosidase inhibition compared to acarbose (IC_{50} = 30.1 μM) (Fig. 31) [80]. Recently, a novel set of quinazolinones having acetamide derivatives was synthesized and screened for their hypoglycemic potential *in vivo* towards STZ-induced hyperglycemic rats. All novel candidates showed hypoglycemic effects especially compound**28**(Fig. 31) which was the most active compound, lowering blood glucose levels by 43.75% [81].

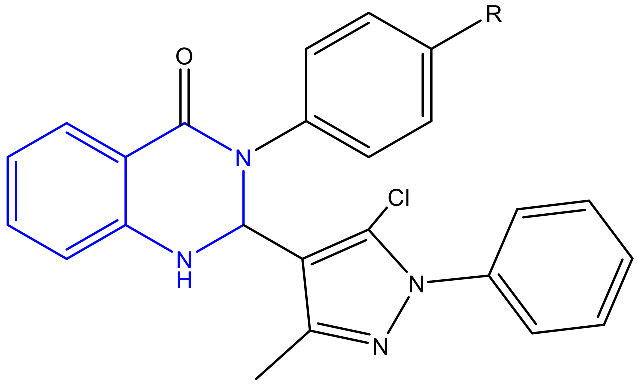

27a, R = OH
27b, R = Cl

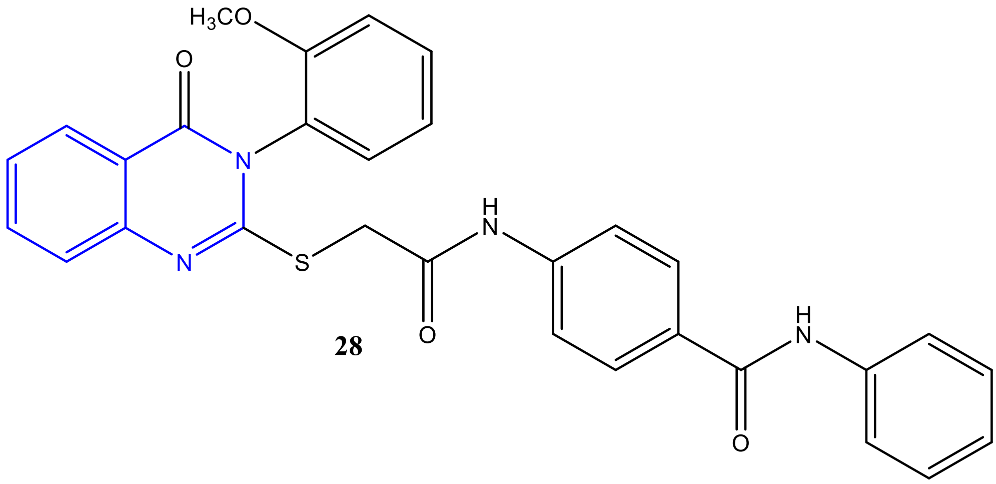

28

Fig. 31. Chemical structures of the antidiabetic quinazolinone derivatives**27a,b**and**28**.

Novel 3-benzyl(phenethyl)-2-thioxobenzo[*g*]quinazoline-4(3*H*)-ones were synthesized in excellent yields by Al-Salahi *et al*[82]. The new derivatives were evaluated for their α-glucosidase inhibitory potential utilizing Baker's yeast α-glucosidase enzyme. All the new benzo[*g*]quinazolines showed α-glucosidase inhibitory effect especially compounds **29**and**30a-d** which revealed better activity than acarbose as listed in Table 8. Structure-activity relationship demonstrated that varying substituents at C-2 and N-3 played prominent roles in the activity profiles as explained in Fig. 32.

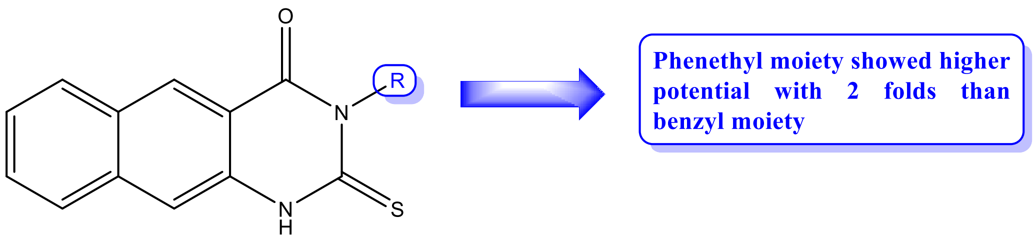

29

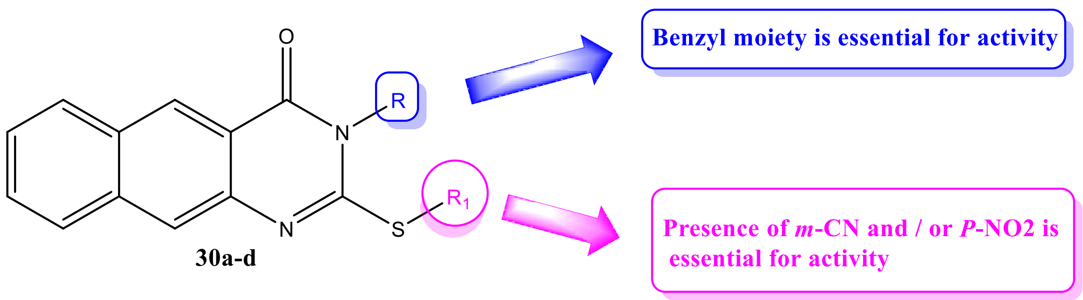

30a-d

Fig.32. SAR study for quinazolinone derivatives **29** and **30a-d** as α-glucosidase inhibitors

Table 8.*α*-Glucosidase inhibitory activity of quinazolinone derivatives **29** and **30a-d**

Compound number	**R**	**R_1**	**IC_{50} (μM)**
29	Phenethyl	--------	69.20 ± 1.76
30a	Benzyl	Benzyl	59.20 ± 0.52
30b	Benzyl	3-CN-benzyl	49.40 ± 0.50
30c	Benzyl	4-NO_2-benzyl	50.20 ± 0.37
30d	Phenethyl	3-CN-benzyl	83.20 ± 0.89
Acarbose	---------------	-----------------	258.27 ± 0.24

The antidiabetic activity for **26b** and **30b** as the most potent quinazoline and quinazolinone derivatives were studied through molecular docking in-silico technique and as α-glucosidase inhibitors. In line with the IC_{50} information given above, compound **26b** displayed higher binding affinity toward α-glucosidase (-8.7 kcal/mol) than **30b** (-8.4 kcal/mol). Fig. 33 shows the interaction of **26b** with α- glucosidase (PDB ID: 3WY1), which is attributed to the conventional hydrogen bonding formed with THR A:226 and ASN A:301, and many hydrophobic interactions like π-σ, π- π T-shaped, alkyl, and π-alkyl, with many residues of the receptor: VAL A:334, PHE A:397, LYS A:398, PRO A:230, and PHE 397.

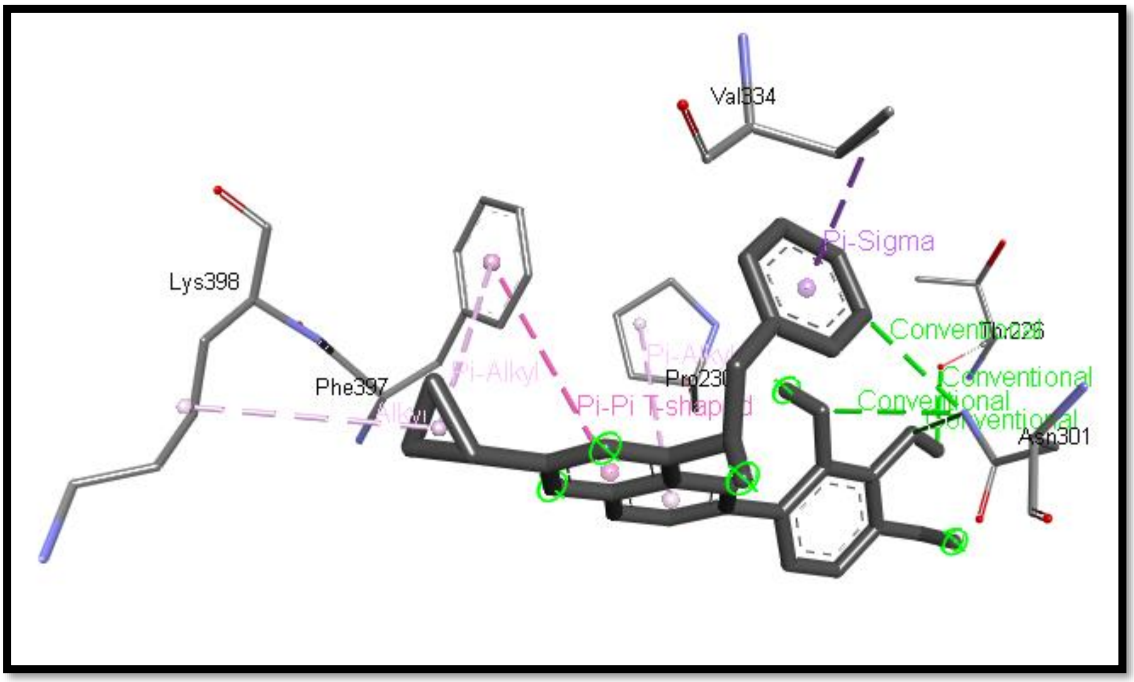

Fig. 33. The binding interactions of **26b** with α-glucosidase (PDB ID: 3WY1)

3.5. Anticonvulsant activity

Many quinazolinone derivatives were FDA-approved for curing epilepsy such as afloqualone (**31**) [83, 84], methaqualone (**32**) [85-89] and mecloqualone (**33**) [90] (Fig.34).

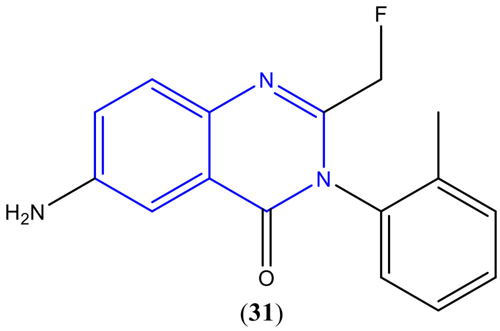

(**31**)

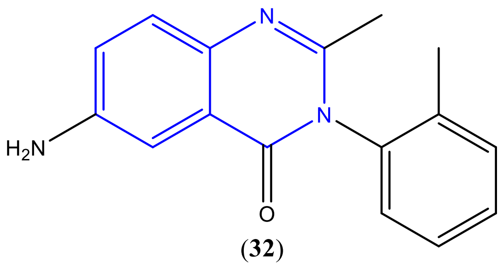

(**32**)

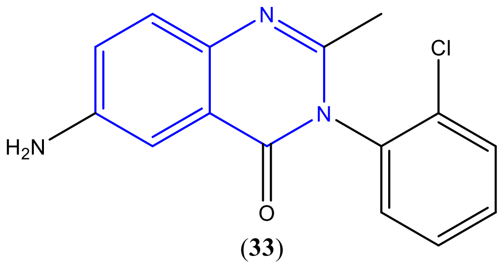

(**33**)

Fig.34. Chemical structures of the approved anticonvulsant quinazolinone derivatives **31-33**.

Furthermore, novel quinazolinone candidates were tested for their anticonvulsant potential[91].The authors designed the target compounds depending on similarities between methaqualone(**31**), mecloqualone (**32**) and the target compounds (**34a-c**). Compounds **34a-c** were 3-4-fold more potent than ethosuximide. SAR study suggested that the butyl group (as a highly lipophilic group) at N-3 plays an essential role in the anticonvulsant activity as in the case of compounds **34a** and**34b**.On the other hand, the benzodiazoxazole moiety at C-2 enhanced the anticonvulsant effect as shown in compound**34c**.The high potential of compounds **34a** and**34b** having electron withdrawing group (Cl) and electron releasing group (OCH_3) due to Cl group increased the lipophilicity (compound **34a**) while OCH_3 (compound **34b**) beneficial for efficiency (Fig. 35).

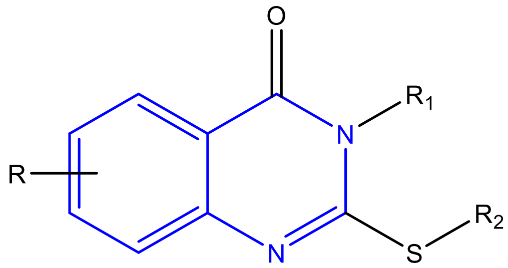

34a, R = methyl, R_1 = butyl, R_2 = 4-Cl-benzyl
34b, R = methyl, R_1 = butyl, R_2 = 3-OCH_3-benzyl
34c, R = methyl, R_1 = benzyl, R_2 = 7-NO_2-benzoxadiazole

Fig. 35. Chemical structures of the anticonvulsant quinazolinone derivatives **34a-c**.

In addition, new diiodo-2-methyl-3-substituted quinazoline-4(3*H*)one derivatives were synthesized and assessed for their anticonvulsant potential[92]. These compounds were designed depending on the chemical structure of methaqualone (**32**). Chemical structure of target compounds **35a-c** fulfilled the pharmacophoric requirements; presence of quinazoline-4-one moiety (hydrophobic part), N (electron donor system), C=O and another hydrophobic distal aryl ring responsible for controlling the pharmacokinetic properties of the anticonvulsant activity. The quinazolinone moiety is linked with the aromatic ring via an aliphatic linker (CH_2) to yield novel compounds having the basic characteristics of methaqualone. Iodine was chosen due to its high tolerance to moisture, nontoxic nature and low cost. From the target compounds, candidates **35a-c** (Fig. 36) showed higher anticonvulsant activity (ED_{50} = 150, 160 and 138 mg/kg, respectively) in comparison with methaqualone (ED_{50} = 200 mg/kg) and valproate (ED_{50} = 300 mg/kg). Structure-activity relationship (SAR) study showed that the anticonvulsant potential was markedly affected by the substitution on the aromatic ring. Electron-withdrawing groups at the aromatic moiety improved the potential more than unsubstituted or electron donating groups.

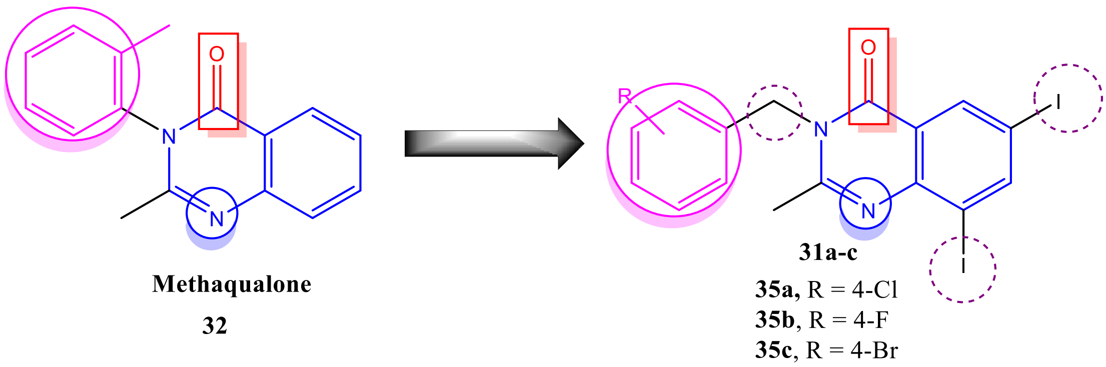

Fig. 36. Rationale design of target quinazolinone derivatives **35a-c**.

One year later, the same group of authors synthesized eight novel quinazolines **36a-h** and assessed them for their anticonvulsant activity using phenytoin as a standard[93]. They modified the chemical structure of **35a-c** by replacing iodine atoms at C-6 and C-8 with fluorine atoms at C-6 as the large size of iodine causes repulsive interaction and negatively affects the binding of iodinated derivatives. From the results, compounds **36e-h**having a halogen atom at the *para* position of the phenyl ring revealed maximum protection towards seizures induced by MES (Table 9). SAR study showed that substituting the phenyl ring with electron donating or electron withdrawing groups had an essential role in their anticonvulsant potential as demonstrated in Fig. 37.

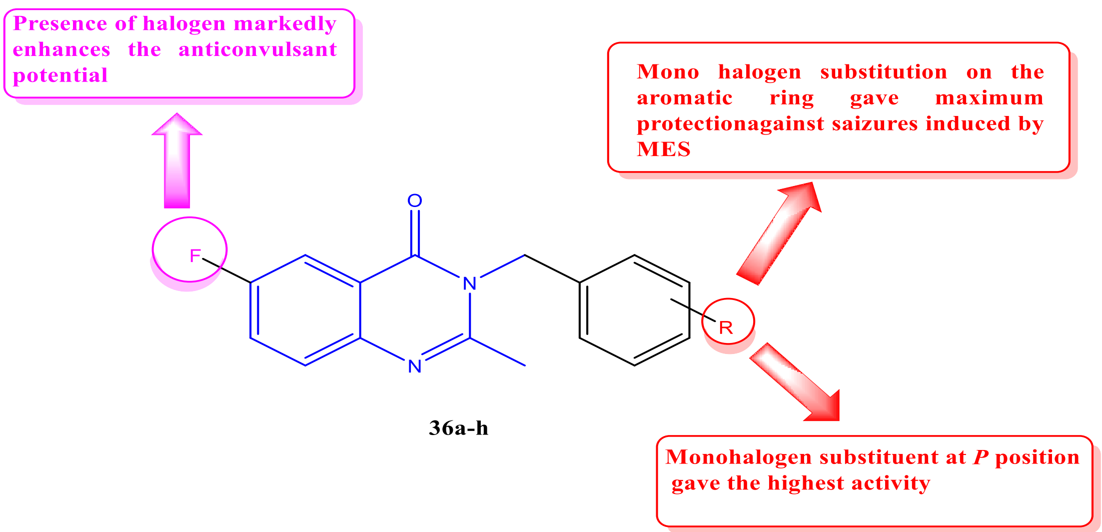

Fig.37. SAR study for 4-quinazolinone derivatives **36a-h** as anticonvulsant agents.

Table 9. Anticonvulsant activity of the target compounds **36a-h** in the maximal electroshock seizure test

Compound number	R	% Protection
36a	H	50.16
36b	4-Cl	71.98
36c	4-F	70.34
36d	4-I	69.48
36e	4-Br	73.07
36f	3-NO_2	53.91
36g	4-OCH_3	25.51
36h	3,5-Cl_2	30.08
Phenytoin	--------------------	78.12

According to reports, drugs used to treat convulsions, epilepsy, and seizures may inhibit hCA. The selection of a specific hCA enzyme as a receptor for molecular docking study was based on previous literature, and the X-ray coordinates of the hCA II isomer from PDB ID: 3F8E were used [91]. Based on the anticonvulsant activity of quinazolines and their protection percentage, the compound **32e** which showed the highest activity was chosen as a ligand for the in-silico study. The free binding energy recorded for **36e** and 3F8E as a receptor was -6.8 kcal/mol and found to be higher than those recorded by Abuelizz*et al*[91]for quinazolines (-3.19 to -4.01 kcal/mol). The higher affinity of **36e** toward 3F8E could be attributed to the conventional hydrogen bond with TYR A:7, carbon-hydrogen bond with PRO A:237, π- π stacked with PHE A:231, π- anion with GLU A:239, and alkyl bonding with PRO A:237 (Fig. 38).

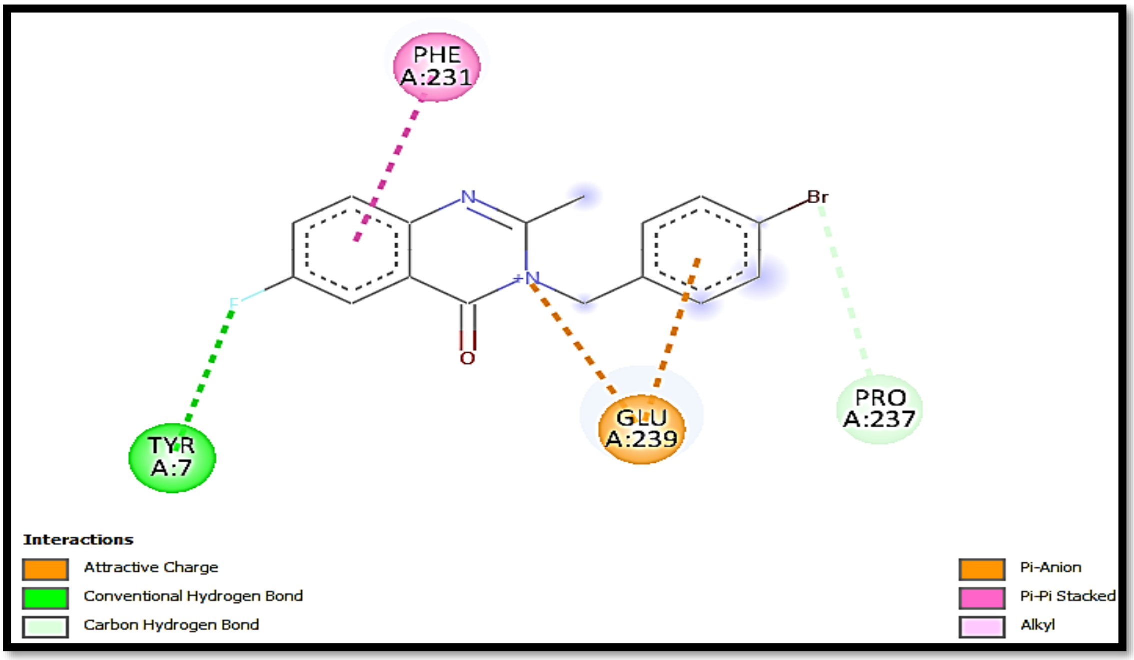

Fig. 38. Docking of quinazoline **36e**in the active site of hCA II (PDB ID: 3F8E).

Moreover, a novel series of *N*-(4-substitutedphenyl)-4-(1-methyl (or 1,2-dimethyl)-4-oxo-1,2-dihydroquinazolin-3(4*H*)-yl)- alkanamides was designed and synthesized as anticonvulsant candidates [94]. All synthesized derivatives revealed good anticonvulsant potential in particular the quinazolinone derivatives **37a-c** (ED_{50} = 28.90-56.40 mg/kg) which recorded superior anticonvulsant potential when compared to phenytoin (ED_{50}> 500 mg/kg) (Fig.39).

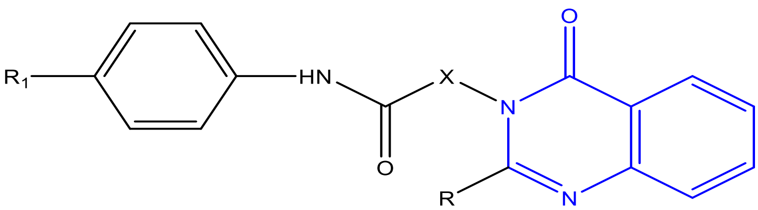

37

Fig. 39; Chemical structure of compounds**37a-c.**

Compound number	R	R_1	X
37a	**H**	**Cl**	**$CHCH_3$**
37b	**H**	**Cl**	**$(CH_2)_3$**
37c	**H**	**F**	**$(CH_2)_3$**

Summary of the SAR of Quinazolinone derivatives as anticonvulsant agents:

SAR analysis of quinazoline derivatives as anticonvulsant agents displayed that aromatic substitution at N-3 is essential for the anticonvulsant activity. Moreover, electron withdrawing group at the aromatic ring enhanced the anticonvulsant potential than the unsubstituted or electron releasing group. Furthermore, the methyl group and substituted methyl group at C-2 is significant for the anticonvulsant activity. Replacing the methyl groups by alkoxymethyl and alkylthiomethyl groups retained the anticonvulsant activity. Presence of halogen markedly improves the anticonvulsant activity as recorded in Fig 40.

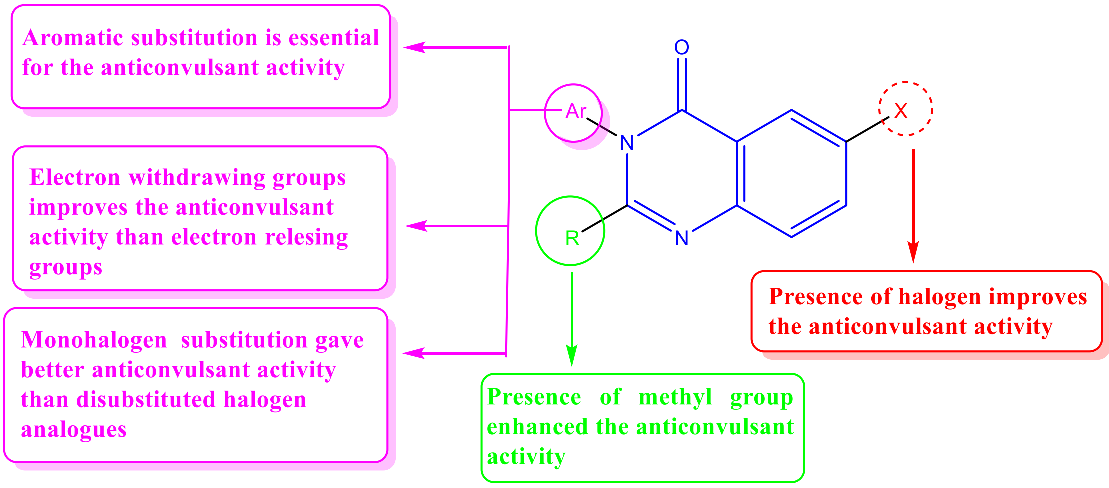

Fig. 40.SAR analysis of quinazolin-4-one derivatives as anticonvulsant agents.

3.6. Antitubercular activity

Novel derivatives of quinazoline-4(3*H*)ones were prepared, designed and evaluated for their antitubercular potential[95]. The obtained results revealed that compounds **38a-e** (Fig. 41) showed excellent antitubercular activity with percentage inhibition of 90-96% at MIC < 6.25 µg/ml. Quinazolinone derivatives having electron- releasing groups (CH_3 and OCH_3) at the ortho position and electronegative group (Cl) at ortho and para positions led to enhancement of activity.

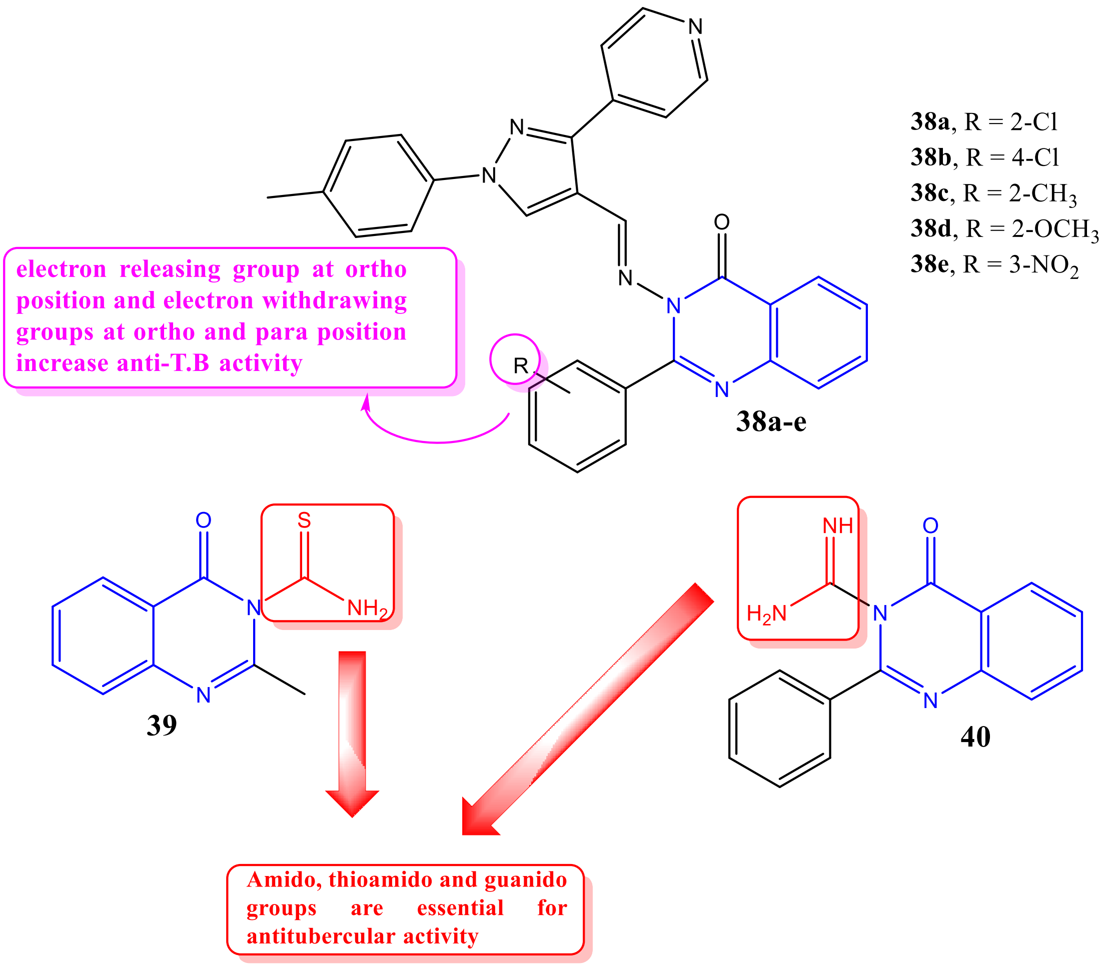

Fig.41. Chemical structures of quinazolinone candidates **38a-e, 39** and **40**.

Sets of 2-methylsubstituted quinazolinone and 2-phenylquinazolinones were prepared and evaluated for their antitubercular activity by Rajasekhar *et al*[96]. 2-Methyl-4-oxoquinazoline carbothioamide derivative **39** and 4-oxo-2-phenylquinazolinecarboximidamide derivative **40** were the most potent candidates with MIC = 6.25 µg/ml. SAR study showed the importance of incorporating amide, guanidino and thioamido groups at 3rd position of quinazolinone nucleus as depicted in Fig. 41. In addition, compound **41**(Fig. 42) was found to inhibit MTB-AHAS with an IC_{50} value equal to 6.50 µM [97]. Acetohydroxyacid synthase (AHAS) with PDB ID: 6BD9 was used as a receptor to study the potential activity of the compound **41** and its affinity to inhibit such enzyme or the receptor. High free binding energy was detected (-9.6 kcal/mol) which revealed the higher affinity of the ligand toward the receptor.

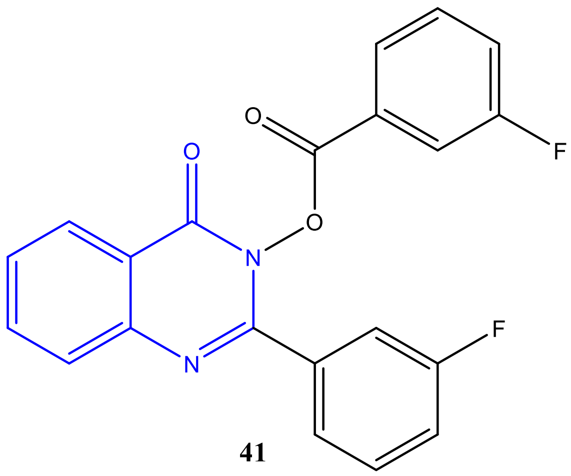

41

Fig. 42. Chemical structure of quinazolinone derivative **41**.

Acetohydroxyacid synthase (AHAS) with PDB ID: 6BD9 was used as a receptor to study the potential activity of compound **41** and its affinity to inhibit such enzyme or the receptor. High free binding energy was detected (-9.6 kcal/mol), which revealed the higher affinity of the ligand toward the receptor. Different conventional hydrogen, carbon-hydrogen, and hydrophobic interactions could be observed in Fig. 43, which are responsible for the higher affinity and may explain the potential antitubercular activity of compound **41** as an AHAS enzyme inhibitor.

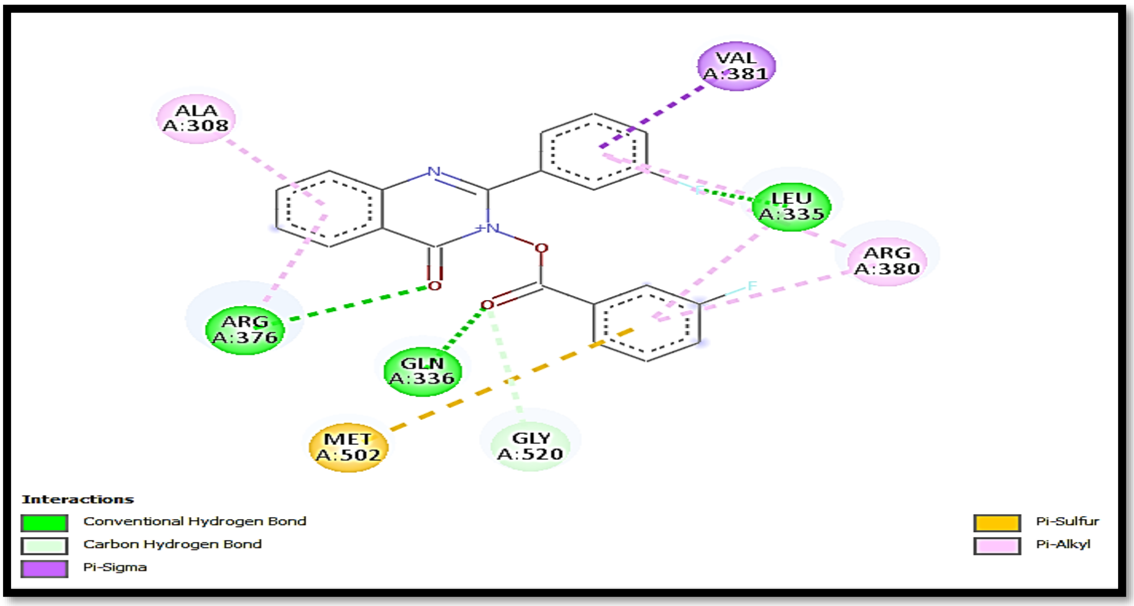

Fig. 43. Molecular docking of the compound **41**and AHAS enzyme (PDB ID: 6BD9).

3.7. Anti-viral activity

New derivatives of quinazolines were prepared and assessed for their antiviral potential towards Dengue virus (DENV) by Venkatesham and co-workers [98]. The rationale of this work is based upon combination between *N*-sulfonylanthranilic acid derivative (**42**) that displayed inhibition of DENV RdRp (IC_{50} = 0.7 µM) and 2,4-diaminoquinazoline derivative (**43**)which revealed high antiviral potency (EC_{50} = 2.8 nM) and an excellent pharmacokinetic profile against DENV (Fig. 44).

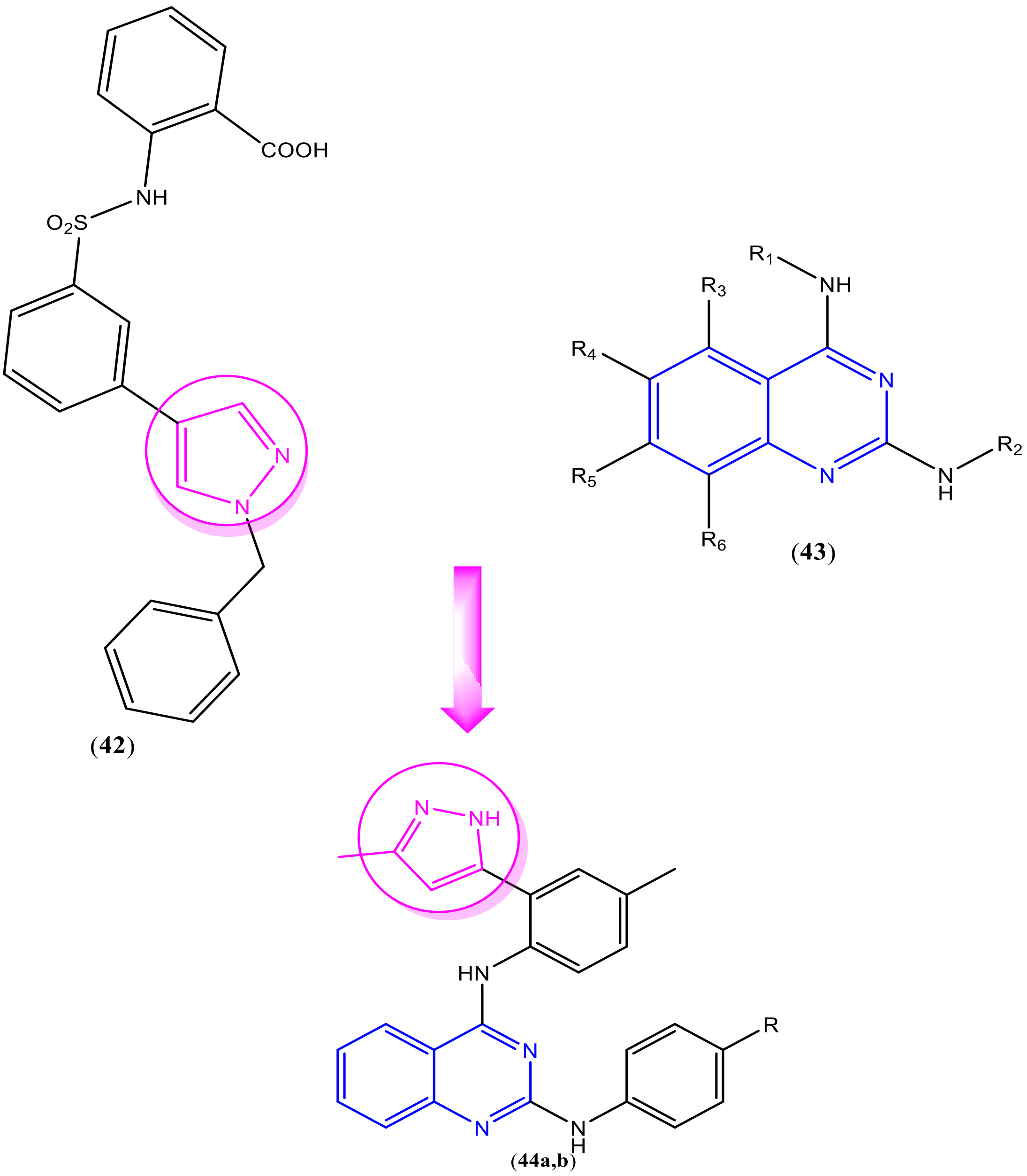

Fig. 44. Rationale design of quinazoline derivatives (**44a,b**) as anti-viral agents.

The quinazoline derivatives **44a,b** comprising the pyrazole moiety revealed strong inhibitory effect on dengue virus proliferation (2.6 µm and 6.7 µm, respectively, based on RNA viral load determination).

Moreover, 2,3,6-trisubstituted quinazolinone derivative (**45**) was identified as inhibitors of ZIKV and Dengue (DENV) inhibitors with EC_{50} = 0.10 µM against ZIKV-FLR, 0.09 µM against ZIKV-HN16, 0.21 µM against DENV-2 and 0.12 µM against DENV-3 (Fig. 45)[99].

Furthermore, new quinazolinone-peptido-nitrophenyl derivatives were prepared and identified as SARS-CoV-2 Main Protease inhibitors [100]. The rationale in this study isbased upon fragment-based strategy of quinazolinone moiety as a potential antiviral and glutamine or glutamate-derived peptidomimetric and positioned nitro functional groups. From the newly prepared quinazolinone derivatives, compounds **46** and **47**(Fig. 45) displayed anti-Main Protease with IC_{50} = 22.47 ± 8.93 µM and 24.04 ± 0.67 µM, respectively.

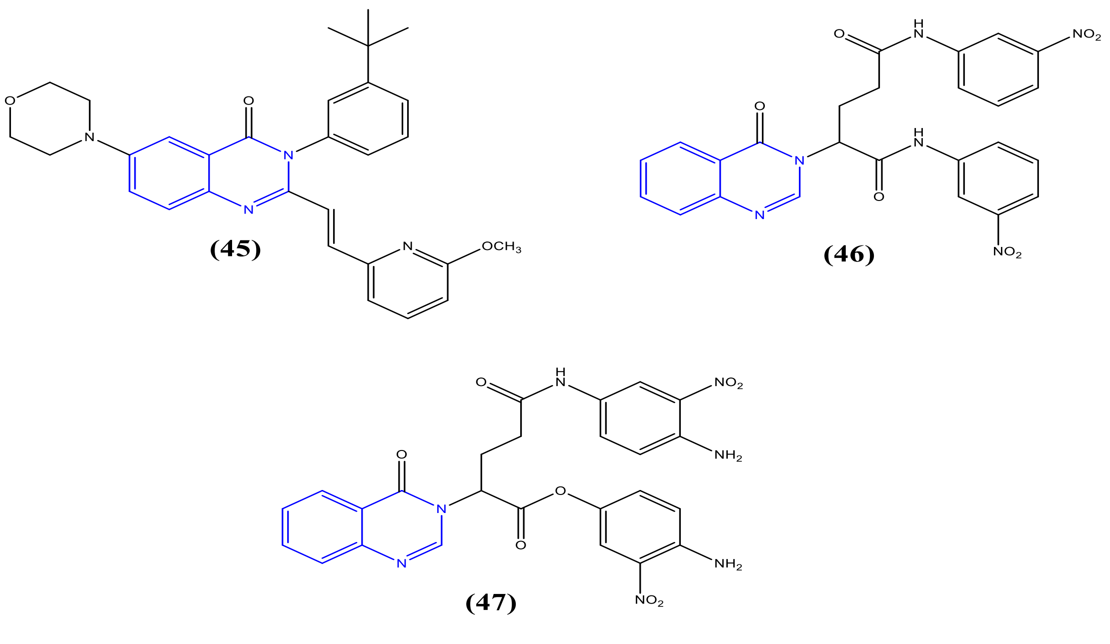

Fig.45. Chemical structures of some quinazolinone derivatives **45-47** as antiviral agents.

New ferulic acid ester derivatives having quinazoline ring were prepared and assessed for their antiviral potential towards tobacco mosaic virus (TMV) and cucumber mosaic virus (CMV) [101]. The authors suggested that the introduction of a quinazoline ring into ferulic acid would produce new derivatives with antiviral activity. Compounds**48a,b** (Fig. 46) showed the same curative activities against CMV (57.2 and 58.1%, respectively) to that exhibited by ningnanmycin (50.5%).In addition, quinazolinone containing some amino acids **49**(Fig. 46) were tested for their antiviral activity against HSV-1 applying CPE inhibition assay. Against a normal Vero cell culture entire derivatives were tested for cytotoxic potency and they concluded that the CTC50 values of all compounds were between 300-420 µg/ml. all the prepared compounds were evaluated at 3 concentration levels (200, 300 and 400 µg/ml) against HSV-1. The proline derivative displayed 90% protection which was equal acyclovir (25µg/ml). Cysteine and glutamic acid derivatives showed 75% protection at concentration 400 µg/ml. other lower dilutions of theabove derivative showed 50% protection only; while lysine and glycine recorded 50% protection only at all dilutions.

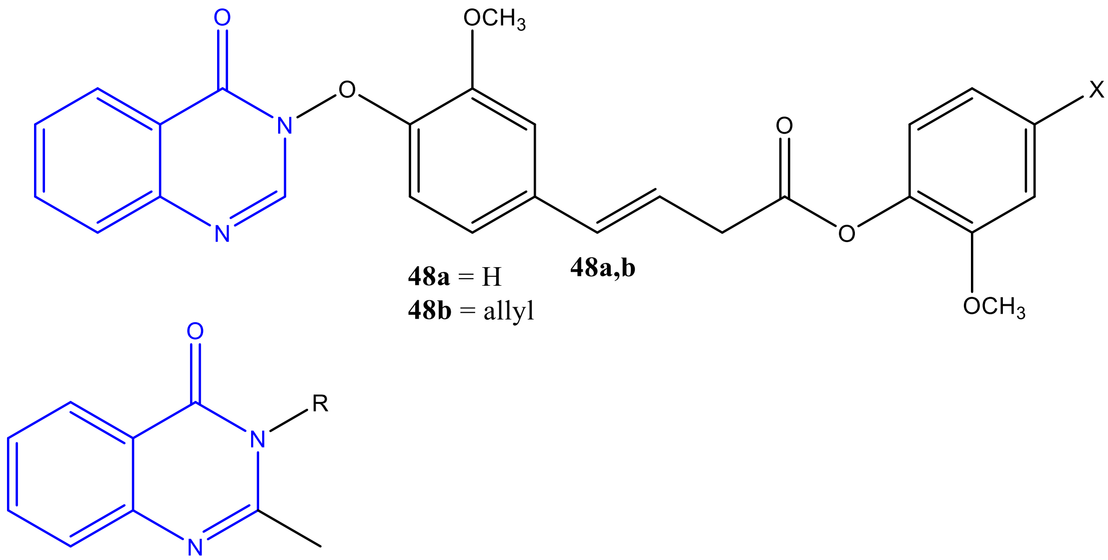

48a = H
48b = allyl
48a,b

49

Fig. 46. Chemical structure of quinazolinone derivatives **48a,b** and **49**.

In 2020, new series of 2,4-disubstitutedquinazoline derivatives were prepared and estimated for their anti-influenza A potential [102]. The rationale of this study based upon bio-isosterism between 3-substituted indoles (**50**) and the quinazoline ring making modifications at C-2 and C-4 at quinazoline ring (Fig. 47). Compound **51** was the most active quinazoline derivative (IC_{50} = 3.17 ± 0.82 µM) and showed 4.1-fold more potency than ribavirin (IC_{50} = 15.36 ± 0.93 µM).

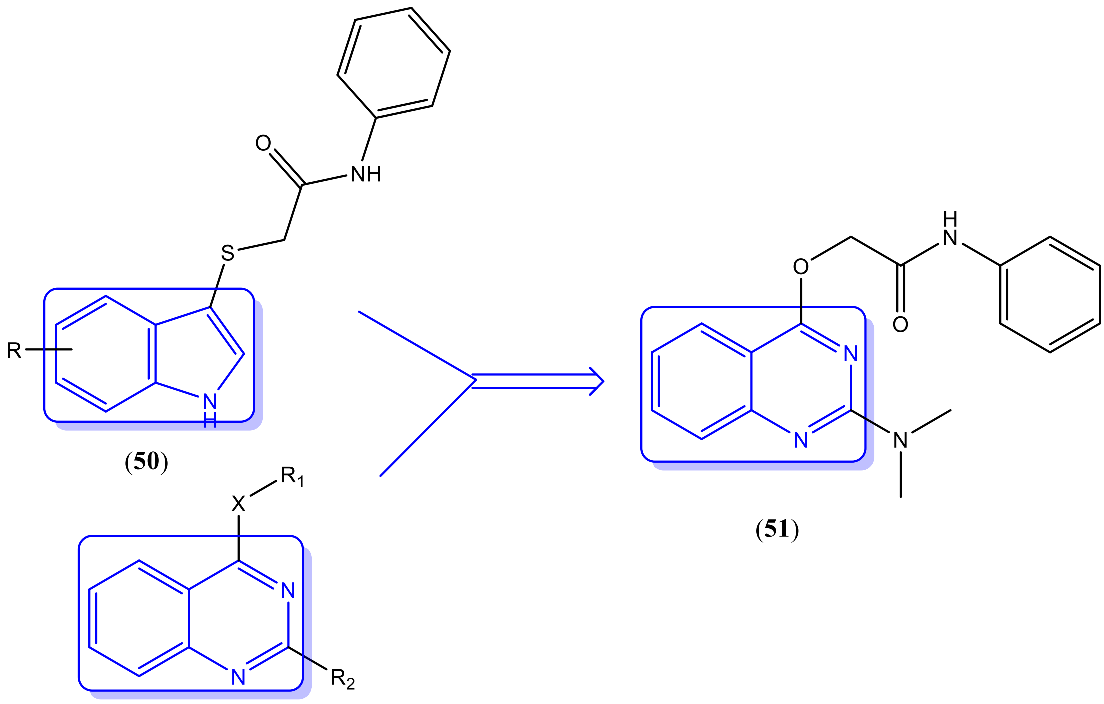

(**50**)

50a

(**51**)

Fig. 47. Rationale design of quinazoline derivative **51** as an antiviral agent.

Furthermore, a new series of quinazoline-4-one having malonate moiety was synthesized and assessed for their antiviral activity towards cucumber mosaic virus (CMV)[103]. The authors performed modifications on diethyl-2-(1-(4-((6-chloropyridin3-yl) methoxy)phenyl)-3-oxo-3-phenylpropyl) malonate (**52**) which showed good antiviral activity towards CMV with EC_{50} = 186.2 µg/ml. This modification comprises replacement 6-chloropyridine moiety with an antiviral ring quinazolin-4-one and interchanging the groups between C-2 and C-4 position of chalcone derivatives as recorded in Fig. 48. Compounds **53a-d** showed excellent curative activities against CMV at 500 µg/mL, with the inhibition rates of 57.1%, 64.3%, 56.9%, and 58.2%, respectively, which were better than that of Ningnanmycin (56.8%) and superior to that of Ribavirin (39.2%).

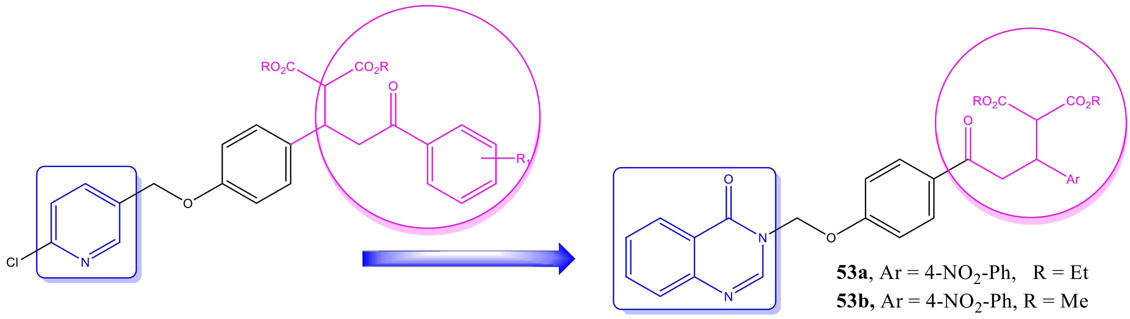

53a, Ar = 4-NO_2-Ph, R = Et
53b, Ar = 4-NO_2-Ph, R = Me
53c, Ar = 3-NO_2-Ph, R =Et
53d, Ar = 3-NO_2-Ph, R = Me

(52) **(53a-d)**

Fig. 48. Rationale design of quinazoline-4-ones having malonate moiety with anti- CMV virus.

3.8. Efflux pump inhibitors

New quinazolinone derivatives were prepared and were found to act as fungal efflux pump inhibitors [104]. The quinazolinone derivative **54** (Fig. 49) was selective for the inhibition of CDR1 in *C. albicans* and CgCDR1 in *C. glabrata*. Moreover, four novel 2-arylquinazoline derivatives **55-58**(Fig. 49) turned out to strongly synergize with CPX at a concentration as low as 0.78 µg/mL against the resistant SA-1199B (norA+), without any effect on wild type SA119[105].

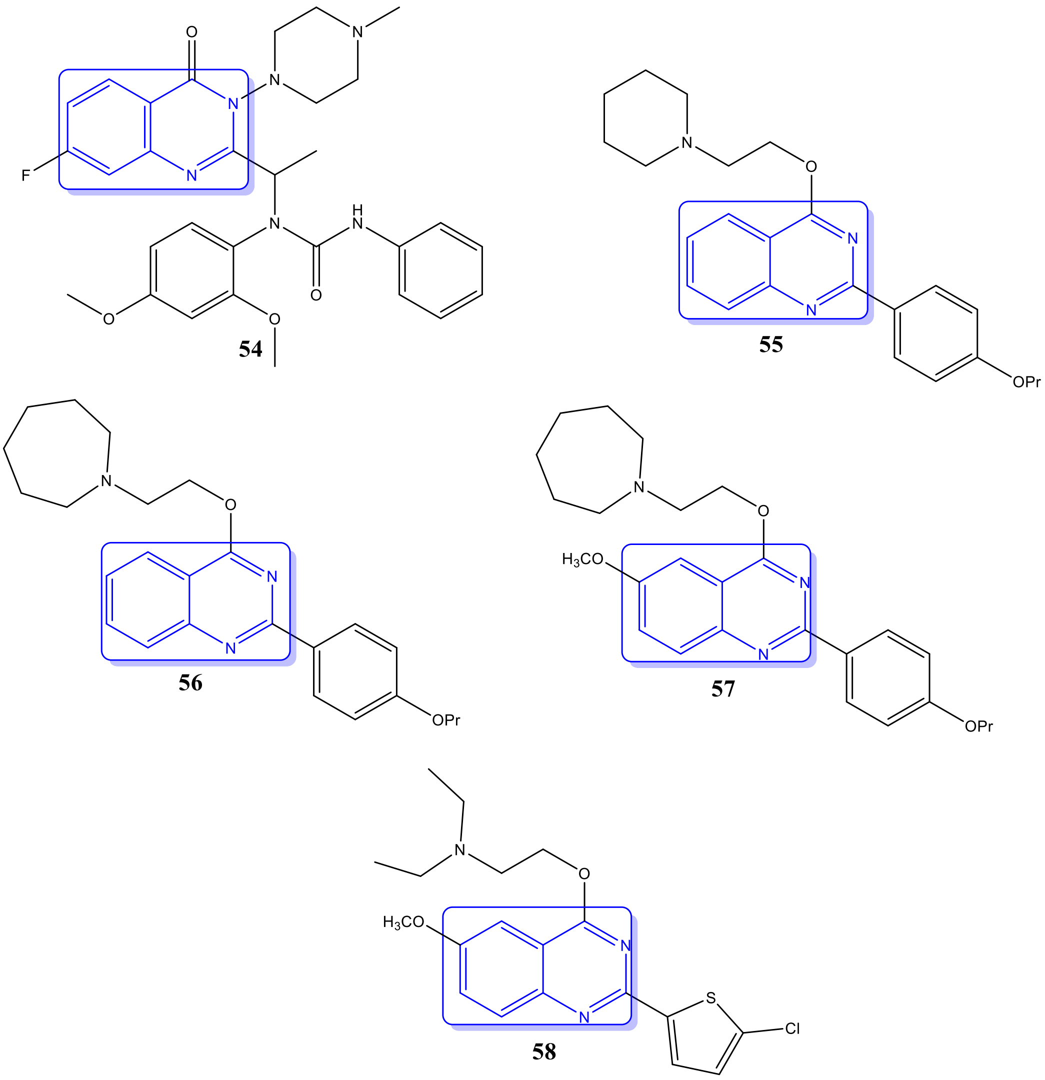

Fig. 49. Chemical structures of quinazoline derivatives **54-58** as efflux pump inhibitors.

4- Conclusion

Various structural modifications of quinazoline and quinazolinone were implemented and evaluated for their pharmacological potential in many diseases. This review shed light on the rationale and many techniques included in the design of quinazoline and quinazolinone derivatives. These privileged scaffolds exhibited diversified pharmacological efficacy as antimicrobial, anticancer, anti-inflammatory, antitubercular, antiviral, efflux pump inhibitors and anticonvulsants. This review certainly provides comprehensive knowledge of structure-activity relationship which will further assist in the development of quinazoline and quinazolinone derivatives with a significant emphasis on treating many fatal diseases.

5- Docking methodology:

The crystal structures of proteins and enzymes used in the molecular docking study were obtained from UniProt (https://www.uniprot.org/, accessed on February 3, 2022) and Protein Data Bank (https://www.rcsb.org/, accessed on December 17, 19, and 24, 2021, August 17, 2022, and June 6-7, 2023). Pymol software (Ver. 2.5.1) was used to prepare the receptors by removing water molecules and co-crystallizing ligands and ions before protonation. Chemdraw was used to create a 2D diagram of the ligands, which was saved in mol format. The 2D structures were converted to 3D and optimized using the MMFF94 force field (Avogadro Software Ver. 1.2.0). Molecular docking was performed by CB-Dock2 (http://clab.labshare.cn/cbdock/php/, accessed on June 5-7 and 10, 2023) which proved to be the most effective technology for blind docking, producing superior interface and visualization profiles for the best-docked complexes**.** The input files were verified and converted to pdbqt format using OpenBabel and MGLTools. AutoDockVina was used for docking, and CB-Dock2 predicted the protein's cavities and determined the centers and dimensions of the top N cavities. The top-ranking poses' RMSD was within 2 Å from the position in the X-ray crystal structure. The best-docked complexes were visualized, and their interface profiles were created using Discovery Studio (Ver. 21.1.0.20298) [106].

Acknowledgement

The authors are thankful to AlMaarefa University for their support.

References

[1] K. Kavitha; N. Yahoob; B. Vijayakumar; K. R. Fathima. *Asian Journal of Research in Chemistry*. **2017**, 10, 577.

[2] G. Agrawal; N. Khan; S. Dwivedi; R. Patel; G. Singh. *Journal of Advanced Scientific Research*. **2021**, 12, 123.

[3] P. Saini; K. Kumar; S. Meena; D. K. Mahawar; A. Dandia; K. Ameta, et al. *N-Heterocycles*. **2022**, 331.

[4] R. A. Mekheimer; M. Abd-Elmonem; M. Abou Elsebaa; M. H. Nazmy; K. U. Sadek. *Physical Sciences Reviews*. **2022**.

[5] M. A. Alanazi; W. A. A. Arafa; I. O. Althobaiti; H. A. Altaleb; R. B. Bakr; N. A. A. Elkanzi. *ACS Omega*. **2022**, 7, 27674.

[6] R. B. Bakr; N. A. Elkanzi; A. A. Ghoneim; S. Moustafa. *Heterocycles: an international journal for reviews and communications in heterocyclic chemistry*. **2018**, 96, 1941.

[7] A. M. Alafeefy; A. A. Kadi; O. A. Al-Deeb; K. E. El-Tahir; N. A. Al-Jaber. *European Journal of Medicinal Chemistry*. **2010**, 45, 4947.

[8] K. Amin; M. Kamel; M. Anwar; M. Khedr; Y. Syam. *European Journal of Medicinal Chemistry*. **2010**, 45, 2117.

[9] M. N. Noolvi; H. M. Patel; V. Bhardwaj; A. Chauhan. *Eur J Med Chem*. **2011**, 46, 2327.

[10] D. Das; L. Xie; J. Wang; X. Xu; Z. Zhang; J. Shi, et al. *Bioorganic & Medicinal Chemistry Letters*. **2019**, 29, 591.

[11] M. A. Abdelgawad; R. B. Bakr; O. A. Alkhoja; W. R. Mohamed. *Bioorganic chemistry*. **2016**, 66, 88.

[12] K. R. Abdellatif; R. B. Bakr. *Medicinal Chemistry Research*. **2021**, 30, 31.

[13] Z. Ali; M. J. Akhtar; M. R. Haider; A. A. Khan; A. A. Siddiqui; M. S. Yar. *Bioorganic chemistry*. **2017**, 71, 181.

[14] Z. Ali; M. J. Akhtar; A. A. Siddiqui; A. A. Khan; M. R. Haider; M. S. Yar. *Arch Pharm (Weinheim)*. **2017**, 350, 1600298.

[15] M. U. Rahman; A. Rathore; A. A. Siddiqui; G. Parveen; M. S. Yar. *Journal of Enzyme Inhibition and Medicinal Chemistry*. **2014**, 29, 733.

[16] Y. Rojas-Aguirre; F. Hernandez-Luis; C. Mendoza-Martinez; C. P. Sotomayor; L. F. Aguilar; F. Villena, et al. *Biochim Biophys Acta*. **2012**, 1818, 738.

[17] S. Shiba; A. El-Khamry; M. Shaban; K. Atia. *Die Pharmazie*. **1997**, 52, 189.

[18] E. Jafari; M. R. Khajouei; F. Hassanzadeh; G. H. Hakimelahi; G. A. Khodarahmi. *Res Pharm Sci*. **2016**, 11, 1.

[19] R. P. Modh; E. De Clercq; C. Pannecouque; K. H. Chikhalia. *Journal of enzyme inhibition and medicinal chemistry*. **2014**, 29, 100.

[20] K. Vijayakumar; A. J. Ahamed; G. Thiruneelakandan. *J Appl Chem*. **2013**, 5.

[21] V. M. Buha; D. N. Rana; M. T. Chhabria; K. H. Chikhalia; B. M. Mahajan; P. S. Brahmkshatriya, et al. *Medicinal Chemistry Research*. **2013**, 22, 4096.

[22] A. S. El-Azab; K. E. ElTahir. *Bioorganic & medicinal chemistry letters*. **2012**, 22, 327.

[23] M. F. Zayed; S. K. Ihmaid; H. E. Ahmed; K. El-Adl; A. M. Asiri; A. M. Omar. *Molecules*. **2017**, 22, 188.

[24] A. A. Mohammadi; S. Taheri; S. Shisheboran; R. Ahdenov; M. Mohammadi-Khanaposhtani; P. S. Darjani, et al. *Journal of Biochemical and Molecular Toxicology*. **2023**, 37, e23234.

[25] M. Sarfraz; N. Sultana; M. I. TARIQ. *Rev Roum Chim*. **2018**, 63, 1035.

[26] M. Sarfraz; N. Sultana; M. I. Tariq; M. Parvez. *Zeitschrift für Kristallographie-Crystalline Materials*. **2019**, 234, 605.

[27] B. Mathew; D. G. Parambi; M. Singh; O. M. Hendawy; M. M. Al-Sanea; R. B. Bakr. Protopine. Naturally Occurring Chemicals Against Alzheimer's Disease: Elsevier; 2021. p. 167.

[28] T. Mohamed; P. P. Rao. *European journal of medicinal chemistry*. **2017**, 126, 823.

[29] G. Saravanan; V. Alagarsamy; C. R. Prakash. *Int J Pharm Pharm Sci*. **2010**, 2, 83.

[30] C. Wattanapiromsakul; P. I. Forster; P. G. Waterman. *Phytochemistry*. **2003**, 64, 609.

[31] S. B. Mhaske; N. P. Argade. *Tetrahedron*. **2006**, 62, 9787.

[32] A. S. Chiriapkin; I. P. Kodonidi; D. I. Pozdnyakov. *Chimica Techno Acta*. **2022**, 9, 20229212.

[33] T. T. Yadav; M. Murahari; G. Peters; M. Yc. *European Journal of Medicinal Chemistry*. **2022**, 114527.

[34] S. Karimian; F. Kazemi; M. Attarroshan; M. Gholampour; S. Hemmati; A. Sakhteman, et al. *BMC chemistry*. **2021**, 15, 1.

[35] P. S. Auti; G. George; A. T. Paul. *RSC Adv*. **2020**, 10, 41353.

[36] K. Haider; S. Das; A. Joseph; M. S. Yar. *Drug Development Research*. **2022**.

[37] Z. Xu. *Eur J Med Chem*. **2020**, 206, 112686.

[38] J. Debray; J. M. Leveque; C. Philouze; M. Draye; M. Demeunynck. *J Org Chem*. **2010**, 75, 2092.

[39] L. Xu; H. Li; Z. Liao; K. Lou; H. Xie; H. Li, et al. *Org Lett*. **2015**, 17, 3434.

[40] U. P. Saikia; G. Borah; P. Pahari. *European Journal of Organic Chemistry*. **2018**, 2018, 1211.

[41] J. Liu; Y.-L. Wang; J.-H. Zhang; J.-S. Yang; H.-C. Mou; J. Lin, et al. *ACS omega*. **2018**, 3, 4534.

[42] R. Sarma; D. Prajapati. *Green chemistry*. **2011**, 13, 718.

[43] D. Z. Wang; L. Yan; L. Ma. *JoVE (Journal of Visualized Experiments)*. **2016**, e53662.

[44] A. Foucourt; D. Hédou; C. Dubouilh-Benard; L. Désiré; A.-S. Casagrande; B. Leblond, et al. *Molecules*. **2014**, 19, 15546.

[45] A. Foucourt; C. Dubouilh-Benard; E. Chosson; C. Corbière; C. Buquet; M. Iannelli, et al. *Tetrahedron*. **2010**, 66, 4495.

[46] H. Luo; D. Hu; J. Wu; M. He; L. Jin; S. Yang, et al. *International Journal of Molecular Sciences*. **2012**, 13, 6730.

[47] W.-H. Lin; W.-C. Wu; M. Selvaraju; C.-M. Sun. *Organic Chemistry Frontiers*. **2017**, 4, 392.

[48] N. Miyaura; K. Yamada; A. Suzuki. *Tetrahedron Letters*. **1979**, 20, 3437.

[49] F. Ke; C. Liu; P. Zhang; J. Xu; X. Chen. *Synthetic Communications*. **2018**, 48, 3089.

[50] K. Zhu; J.-H. Hao; C.-P. Zhang; J. Zhang; Y. Feng; H.-L. Qin. *RSC Advances*. **2015**, 5, 11132.

[51] C. L. Jagani; N. A. Sojitra; S. F. Vanparia; T. S. Patel; R. B. Dixit; B. C. Dixit. *Arkivoc*. **2011**, 9, 221.

[52] S. S. Patil; S. D. Jadhav; M. Deshmukh. *Journal of Chemical Sciences*. **2012**, 124, 1043.

[53] W.-L. SHANG; J.-M. ZHANG; J.-A. JIN; X.-L. CHEN. *Chinese Journal of Organic Chemistry*. **2011**, 31, 1272.

[54] M. M. Heravi; M. Ghavidel; L. Mohammadkhani. *RSC advances*. **2018**, 8, 27832.

[55] T. Deligeorgiev; S. Kaloyanova; A. Vasilev; J. J. Vaquero; J. Alvarez-Builla; A. M. Cuadro. *Coloration Technology*. **2010**, 126, 24.

[56] N. Kumar; P. Dubey. **2012**.

[57] A. A. Mohammadi; S. Sadat Hossini. *Chinese Journal of Chemistry*. **2011**, 29, 1982.

[58] R. B Bakr; A. BM Mehany; K. RA Abdellatif. *Anti-Cancer Agents in Medicinal Chemistry (Formerly Current Medicinal Chemistry-Anti-Cancer Agents)*. **2017**, 17, 1389.

[59] R. B. Bakr; A. Mehany. *Molbank*. **2016**, 2016, M915.

[60] S. Mowafy; A. Galanis; Z. M. Doctor; R. M. Paranal; D. S. Lasheen; N. A. Farag, et al. *Bioorg Med Chem*. **2016**, 24, 3501.

[61] A. J. Ansari; G. Joshi; U. P. Yadav; A. K. Maurya; V. K. Agnihotri; S. Kalra, et al. *Bioorganic Chemistry*. **2019**, 93, 103314.

[62] A. Farouk; T. Alsulami; H. S. Ali; A. N. Badr. *Toxins (Basel)*. **2023**, 15.

[63] M. Zou; B. Jin; Y. Liu; H. Chen; Z. Zhang; C. Zhang, et al. *Letters in Drug Design & Discovery*. **2019**, 16, 102.

[64] W. Hou; Y. Ren; Z. Zhang; H. Sun; Y. Ma; B. Yan. *Bioorganic & Medicinal Chemistry*. **2018**, 26, 1740.

[65] S. Thakral; D. Saini; A. Kumar; N. Jain; S. Jain. *Medicinal Chemistry Research*. **2017**, 26, 1595.

[66] S. El-Sayed; K. Metwally; A. A. El-Shanawani; L. M. Abdel-Aziz; H. Pratsinis; D. Kletsas. *Chem Cent J*. **2017**, 11, 102.

[67] G. Le-Nhat-Thuy; T. Van Dinh; H. Pham-The; H. N. Quang; N. N. Thi; T. A. D. Thi, et al. *Bioorganic & Medicinal Chemistry Letters*. **2018**, 28, 3741.

[68] J. Hu; Y. Zhang; L. Dong; Z. Wang; L. Chen; D. Liang, et al. *Chemical Biology & Drug Design*. **2015**, 85, 672.

[69] G. Saravanan; V. Alagarsamy; P. Dineshkumar. *Archives of Pharmacal Research*. **2021**, 44, 1.

[70] B. Dash; S. Dash; D. Laloo; C. Medhi. *Journal of Applied Pharmaceutical Science*. **2017**, 7, 083.

[71] P. M. Chandrika; T. Yakaiah; A. R. R. Rao; B. Narsaiah; N. C. Reddy; V. Sridhar, et al. *European journal of medicinal chemistry*. **2008**, 43, 846.

[72] B. Ghodge; A. Kshirsagar; V. Navghare. *Beni-Suef University Journal of Basic and Applied Sciences*. **2020**, 9, 1.

[73] A. Aouf; S. Bouaouina; M. A. Abdelgawad; M. A. S. Abourehab; A. Farouk. *Antibiotics (Basel)*. **2022**, 11.

[74] R. Ferreira de Freitas; M. Schapira. *Medchemcomm*. **2017**, 8, 1970.

[75] N. C. Desai; K. A. Jadeja; D. J. Jadeja; V. M. Khedkar; P. C. Jha. *Synthetic Communications*. **2021**, 51, 952.

[76] A. Farouk; A. G. Abdel-Razek; K. Gromadzka; A. N. Badr. *Plants (Basel)*. **2022**, 11.

[77] R. S. Gouhar; M. M. Kamel. *Journal of Heterocyclic Chemistry*. **2018**, 55, 2082.

[78] T. Rekha; S. Durgamma; A. Padmaja; V. Padmavathi. *Monatshefte für Chemie-Chemical Monthly*. **2017**, 148, 1781.

[79] V. Gurram; R. Garlapati; C. Thulluri; N. Madala; K. S. Kasani; P. K. Machiraju, et al. *Medicinal Chemistry Research*. **2015**, 24, 2227.

[80] A. Barmak; K. Niknam; G. Mohebbi. *ACS Omega*. **2019**, 4, 18087.

[81] A. Ibrahim; H. M. Sakr; R. R. Ayyad; M. M. Khalifa. *ChemistrySelect*. **2022**, 7, e202104590.

[82] R. Al-Salahi; R. Ahmad; E. Anouar; N. I. Iwana Nor Azman; M. Marzouk; H. A. Abuelizz. *Future medicinal chemistry*. **2018**, 10, 1889.

[83] L. Hroch; L. Aitken; O. Benek; M. Dolezal; K. Kuca; F. Gunn-Moore, et al. *Current Medicinal Chemistry*. **2015**, 22, 730.

[84] R. I. Cohen; C. A. Warfield. Role of muscle relaxants in the treatment of pain. Treatment of Chronic Pain by Medical Approaches: Springer; 2015. p. 67.

[85] M. Ionescu-Pioggia; M. Bird; M. H. Orzack; F. Benes; B. Beake; J. O. Cole. *Int Clin Psychopharmacol*. **1988**, 3, 97.

[86] A. G. Alhamzani; T. A. Yousef; M. M. Abou-Krisha; M. Raghu; K. Y. Kumar; M. Prashanth, et al. *Bioorganic & Medicinal Chemistry Letters*. **2022**, 77, 129042.

[87] H. N. Deepakumari; B. K. Jayanna; M. K. Prashanth; H. D. Revanasiddappa; B. Veeresh. *Arch Pharm (Weinheim)*. **2016**, 349, 566.

[88] M. F. Zayed; H. E. Ahmed; A.-S. M. Omar; A. S. Abdelrahim; K. El-Adl. *Medicinal Chemistry Research*. **2013**, 22, 5823.

[89] K. Wilson; M. Oram; C. E. Horth; D. Burnett. *Br J Clin Pharmacol*. **1982**, 14, 333.

[90] M.-K. Ibrahim; K. El-Adl; A. A. Al-Karmalawy. *Bulletin of Faculty of Pharmacy, Cairo University*. **2015**, 53, 101.

[91] H. A. Abuelizz; R. El Dib; M. Marzouk; E.-H. Anouar; Y. A. Maklad; H. N. Attia, et al. *Molecules*. **2017**, 22, 1094.

[92] M. F. Zayed; H. E. Ahmed; A.-S. M. Omar; A. S. Abdelrahim; K. El-Adl. *Medicinal Chemistry Research*. **2013**, 22, 5823.

[93] M. F. Zayed. *Journal of Taibah University Medical Sciences*. **2014**, 9, 104.

[94] N. A. Noureldin; H. Kothayer; E. M. Lashine; M. M. Baraka; W. El-Eraky; S. A. Awdan. *Arch Pharm (Weinheim)*. **2017**, 350, 1600332.

[95] U. Pandit; A. Dodiya. *Medicinal Chemistry Research*. **2013**, 22, 3364.

[96] K. Rajasekhar; N. Nizamuddin; A. S. Surur; Y. T. Mekonnen. *Research and Reports in Medicinal chemistry*. **2016**, 6, 15.

[97] W. Lu; I. A. Baig; H.-J. Sun; C.-J. Cui; R. Guo; I.-P. Jung, et al. *European Journal of Medicinal Chemistry*. **2015**, 94, 298.

[98] A. Venkatesham; M. Saudi; S. Kaptein; J. Neyts; J. Rozenski; M. Froeyen, et al. *European Journal of Medicinal Chemistry*. **2017**, 126, 101.

[99] M. Ashraf-Uz-Zaman; X. Li; Y. Yao; C. B. Mishra; B. K. Moku; Y. Song. *Journal of Medicinal Chemistry*. **2023**, 66, 10746.

[100] H.-N.-H. Giang; F.-P. Chou; C.-Y. Chen; S.-C. Chou; S.-C. Huang; T. Wu, et al. *Viruses*. **2023**, 15, 287.

[101] Z. Wu; J. Zhang; J. Chen; J. Pan; L. Zhao; D. Liu, et al. *Pest management science*. **2017**, 73, 2079.

[102] M. Wang; G. Zhang; Y. Wang; J. Wang; M. Zhu; S. Cen, et al. *Bioorganic & Medicinal Chemistry Letters*. **2020**, 30, 127143.

[103] M. Chen; P. Li; D. Hu; S. Zeng; T. Li; L. Jin, et al. *Bioorganic & Medicinal Chemistry Letters*. **2016**, 26, 168.

[104] W. J. Watkins; R. C. Lemoine; L. Chong; A. Cho; T. E. Renau; B. Kuo, et al. *Bioorganic & Medicinal Chemistry Letters*. **2004**, 14, 5133.

[105] N. Cedraro; R. Cannalire; A. Astolfi; G. Mangiaterra; T. Felicetti; S. Vaiasicca, et al. *ChemMedChem*. **2021**, 16, 3044.

[106] M. E. Shaker; H. A. Goma; I. Alsalahat; N. A. Elkanzi; A. A. Azouz; M. S. Abdel-Bakky, et al. *Journal of Biomolecular Structure and Dynamics*. 1.